Molecular Therapy
Original Article

Exploiting the tumor-suppressive activity of the androgen receptor by CDK4/6 inhibition in castration-resistant prostate cancer

Wanting Han,[1,2] Mingyu Liu,[1,2] Dong Han,[1] Anthia A. Toure,[1,2] Muqing Li,[1,2] Anna Besschetnova,[1,2] Zifeng Wang,[1,2] Susan Patalano,[1,2] Jill A. Macoska,[1,2] Hung-Ming Lam,[3] Eva Corey,[3] Housheng Hansen He,[4,5] Shuai Gao,[1,2] Steven P. Balk,[6] and Changmeng Cai[1,2]

[1]Center for Personalized Cancer Therapy, University of Massachusetts, Boston, Boston, MA 02125, USA; [2]Department of Biology, University of Massachusetts Boston, Boston, MA 02125, USA; [3]Department of Urology, University of Washington, Seattle, WA 98195, USA; [4]Department of Medical Biophysics, University of Toronto, Toronto, ON M5G1L7, Canada; [5]Princess Margaret Cancer Center, University Health Network, Toronto, ON M5G1L7, Canada; [6]Hematology-Oncology Division, Department of Medicine, Beth Israel Deaconess Medical Center and Harvard Medical School, Boston, MA 02215, USA

The androgen receptor (AR) plays a pivotal role in driving prostate cancer (PCa) development. However, when stimulated by high levels of androgens, AR can also function as a tumor suppressor in PCa cells. While the high-dose testosterone (high-T) treatment is currently being tested in clinical trials of castration-resistant prostate cancer (CRPC), there is still a pressing need to fully understand the underlying mechanism and thus develop treatment strategies to exploit this tumor-suppressive activity of AR. In this study, we demonstrate that retinoblastoma (Rb) family proteins play a central role in maintaining the global chromatin binding and transcriptional repression program of AR and that Rb inactivation desensitizes CRPC to the high-dose testosterone treatment *in vitro* and *in vivo*. Using a series of patient-derived xenograft (PDX) CRPC models, we further show that the efficacy of high-T treatment can be fully exploited by a CDK4/6 inhibitor, which strengthens the chromatin binding of the Rb-E2F repressor complex by blocking the hyperphosphorylation of Rb proteins. Overall, our study provides strong mechanistic and preclinical evidence on further developing clinical trials to combine high-T with CDK4/6 inhibitors in treating CRPC.

INTRODUCTION

Androgens exert their actions by binding to the androgen receptor (AR) and thus induce the transcriptional activity of AR.[1] While AR is well known for its transcriptional activation function in normal prostate and prostate cancer (PCa) cells, it can also function as a transcriptional repressor by recruiting repressive cofactors (such as LSD1 and EZH2) to suppress the expression of a subset of genes, including *AR* and its splice variants (*AR-Vs*), androgen synthetic genes, and genes mediating DNA replication and repair.[2-5] The transcriptional repression of *AR* and *AR-Vs* and androgen synthetic genes (such as *AKR1C3* and *HSD17B6*) functions as a negative-feedback loop and plays a critical role to restore AR signaling during tumor progression to the castration-resistant stage of PCa (CRPC).[1] More importantly, the repression activity of AR on DNA synthesis and cell-cycle pathways provides a molecular mechanism for the high-dose testosterone (high-T) therapy in PCa.[5,6] Previous studies have shown that high-T treatment alone or in combination with DNA-damaging reagents can suppress the growth of CRPC or CRPC that is resistant to enzalutamide in preclinical studies using patient-derived xenograft (PDX) models.[7,8] Clinical studies of the bipolar androgen therapies (BATs) that periodically treat the CRPC patients with rapid cycling of high-T and AR-signaling-inhibition agents to disrupt the adaptive regulation of AR signaling in CRPC patients also show encouraging results in recent phase II clinical trials.[9-11] Several additional mechanisms have been suggested, including androgen-stimulated DNA-damaging effect, licensing factor function of AR on DNA replication, androgen-induced expression of tumor suppressor genes (such as *ZBTB16*), and androgen-repressed expression of oncogenes (such as *MYC*) and anti-apoptotic proteins.[7,12-19] Nonetheless, there is an urgent need to fully understand the tumor suppressor activity of AR and thus identify treatment strategies that can further exploit the anti-tumor activity of high-dose androgens.

Retinoblastoma protein (Rb) (encoded by *RB1* gene) is a well-established tumor-suppressor protein by forming a repressor complex with E2F transcription factors.[20] The Rb-E2F complex plays an important role in cells to repress the transcription of genes mediating DNA synthesis and cell cycle progression. Hyperphosphorylation of Rb by cyclin D-CDK4/6 and cyclin E-CDK2 disrupts the interaction of Rb with E2Fs and thus activates E2F transcriptional activities.[21] Recent sequencing studies in CRPC tumor samples have revealed a high frequency of *RB1* deletion in ~10%–15% of tumors, and the loss of *RB1* is associated with worse patient outcomes,[22,23] indicating

Received 6 August 2021; accepted 28 January 2022;
https://doi.org/10.1016/j.ymthe.2022.01.039.

Correspondence: Changmeng Cai, PhD, Center for Personalized Cancer Therapy, University of Massachusetts, Boston, Boston, MA 02125, USA.
E-mail: changmeng.cai@umb.edu

a critical role of Rb in preventing the progression of CRPC. *RB1* loss leads to an expansion of E2F1 cistrome, increased redox metabolism, and lineage plasticity, and is associated with the resistance to AR-signaling-inhibition therapies.[24-28] Our previous studies have shown that AR can recruit hypophosphorylated Rb to DNA replication gene loci and strengthens the activity of Rb-E2F suppressor complex.[5] However, it is still unclear how Rb globally mediates this transcriptional repressor activity of AR in CRPC and whether enhancing Rb-E2F transcriptional repression activity can exploit the tumor-suppressive function of high-T *in vivo*.

In this study, using integrated transcriptomic and cistromic analyses, we found that Rb depletion in CRPC cells broadly compromised the AR-mediated direct transcriptional repression on E2F-regulated genes, but not the indirect repression on Myc-regulated genes. We then demonstrated that the Rb-like pocket protein p130 can similarly mediate the transcriptional repression activity of AR and partially compensate for the function of Rb. Moreover, we also found that Rb depletion can reprogram the transcriptional repression activity of AR by altering AR chromatin binding. Consistent with these mechanistic studies, the Rb-proficient CRPC cells were more sensitive to the high-T treatment *in vitro* and *in vivo* in comparison with Rb-deficient cells. Since Rb/p130 activities are highly dependent on CDK4/6, we next determined whether high-T treatment can be combined with CDK4/6 inhibitors. Significantly, we found that a clinically approved CDK4/6 inhibitor, palbociclib, can enhance the efficacy of high-T treatment in a set of CRPC cell line and PDX models. Overall, this study demonstrates a critical role of Rb family proteins in mediating the tumor-suppressive activity of high-T and suggests a therapeutic strategy to enhance the efficacy of high-T treatment with combined treatment of CDK4/6 inhibitors.

RESULTS

High-dose androgen treatment enhances global Rb binding to suppress E2F signaling

Our previous study has shown that AR can transcriptionally repress genes mediating DNA synthesis through direct chromatin binding and the interaction with hypophosphorylated Rb.[5] Therefore, we hypothesize that the AR-promoted Rb-E2F repressor complex activity is a major mechanism for the tumor-suppressive function of high-T in PCa. To further study the role of Rb in this process, we generated a stable cell line expressing doxycycline-inducible lentiviral short hairpin RNA (shRNA) against *RB1* in LNCaP-derived C4-2 CRPC cells (C4-2-tet-shRB).[29] Consistent with the previous studies in VCaP model,[2,30] while 0.1 nM dihydrotestosterone (DHT) treatment can sufficiently activate classic androgen-induced genes, higher concentrations of DHT (>1 nM) were required to induce AR-mediated transcription repression on previously identified DNA synthesis and cell cycle genes in C4-2 model (Figures S1A and S1B). We then globally characterized the transcriptional repression activity of AR in Rb-positive CRPC cells by comparing the high-dose-androgen (10 nM DHT, comparable to the androgen levels in pre-castrated men)-induced AR transcriptome in uninduced C4-2-tet-shRB cells, VCaP cells, and VCaP-CR cells (derived from castration-resistant VCaP xenograft).[2,31] While androgen-induced genes were enriched primarily in lipid biosynthesis pathways (Figure S2A), consistent with previous studies,[32,33] androgen-repressed genes were highly enriched in E2F and Myc transcriptional target gene sets (Figures 1A and 1B and S2B). Both pathways are known to mediate DNA synthesis and cell cycle progression. Interestingly, androgen-repressed genes were also enriched for a previously identified gene set (NE-up) that is upregulated in the neuroendocrine (NE) subtype of CRPC (NEPC),[34] suggesting that AR may transcriptionally repress NE differentiation, a consistent finding with previous studies.[16,35-37] Moreover, combining the chromatin immunoprecipitation sequencing (ChIP-seq) analyses in these models with the transcriptome data, we found that those AR-repressed genes associated with nearby AR bindings (potentially AR directly repressed genes) were similarly enriched for E2F targets and NE-up genes but less enriched for Myc targets (Figure 1C), suggesting that E2F target genes, as well as NE genes, are the major direct targets of AR-mediated transcriptional repression. However, the androgen-repressed expression of Myc target genes is likely an indirect effect that is possibly mediated through repression of the *MYC* gene[15,18] or other Myc cofactors. Consistent with previous findings, AR directly activated genes were enriched for lipid biosynthesis pathways (Figure S2C).[2,33]

Next, we determined whether androgen treatment may globally affect Rb or c-Myc chromatin binding. ChIP-seq analyses of Rb and c-Myc were conducted in C4-2 cells in the absence or presence of 10 nM DHT. As shown in Figures 1D and 1E, the number and intensity of Rb binding peaks were noticeably increased by the androgen treatment, consistent with our previous findings that AR can recruit Rb to strengthen the Rb-E2F repressor complex. However, although the number of c-Myc chromatin binding peaks was increased, the intensity of those binding peaks did not appear to be significantly affected (Figures 1F and 1G). Furthermore, using binding and expression target analysis (BETA),[38,39] we found that Rb chromatin binding was highly associated with the transcriptional repression function of AR, while c-Myc binding was not significantly associated with AR-regulated genes (Figure 1H). Together, these data indicate that AR can directly repress E2F signaling and indirectly repress Myc signaling and that the direct regulation of Rb-E2F activity may be one primary mechanism of AR-mediated transcriptional repression function in CRPC cells.

Rb mediates AR repression of E2F signaling and cell cycle progression

The protein expression of Rb was efficiently depleted by the doxycycline treatment (within 3 days) in C4-2-tet-shRB cells (Figures 2A and S3A), and this Rb ablation impaired the androgen-repressed cell cycle progression (Figure 2B). We then performed RNA-seq analyses in these stable cells with both short-term (3 days) and long-term (~30 days) treatments of doxycycline. As shown in Figures 2C and S3B, while Rb depletion did not appear to broadly affect DHT-induced gene expression, it clearly impaired the repression activity of DHT on a large subset of genes (clusters 1 and 3). We then compared the effect of Rb depletion on the E2F pathway versus the Myc pathway genes. As shown in Figures 2D (upper panel) and

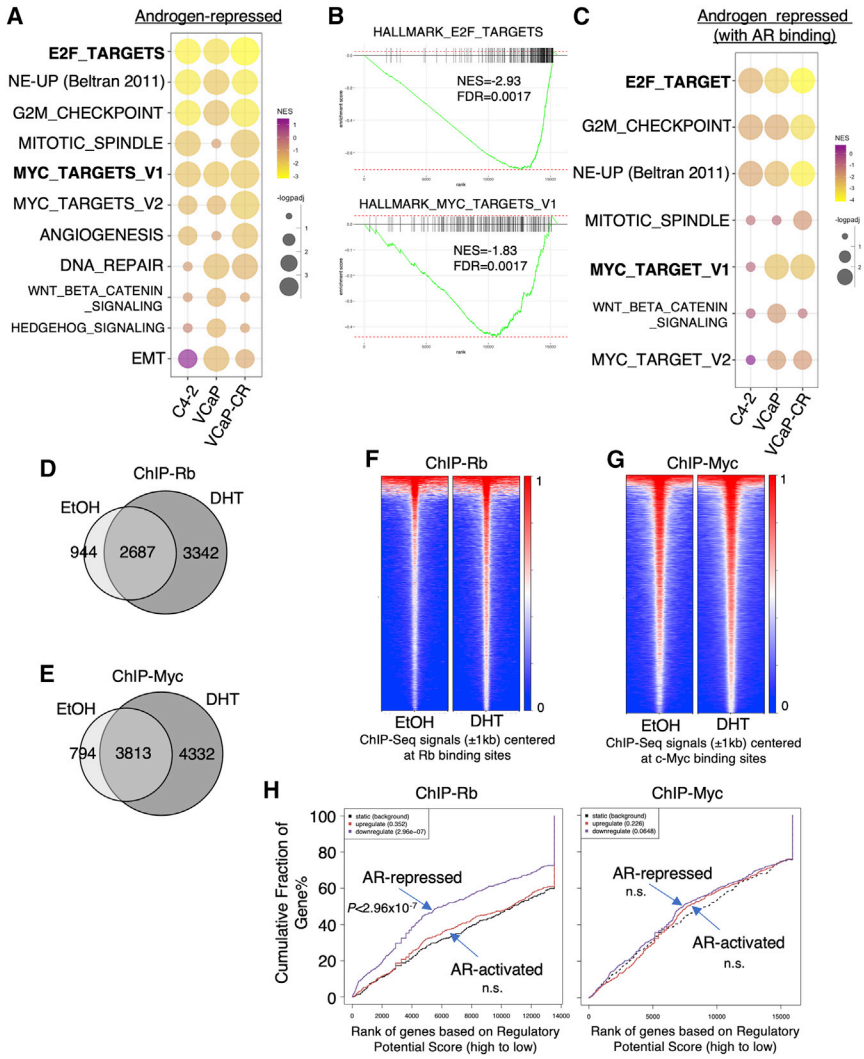

Figure 1. High-dose androgen treatment enhances global Rb binding to suppress E2F signaling

(A) C4-2 cells were stably infected by doxycycline-inducible lentiviral shRNA against non-target control (shNTC) or *RB1* (shRB, C4-2-tet-shRB). RNA-seq was done in C4-2-tet-shRB cells (no doxycycline treatment) stimulated by ethanol or 10 nM DHT for 24 h (hours). The gene profiling data for VCaP and VCaP-CR cells stimulated by ethanol and DHT (10 nM, 24 h) were obtained from a previous study.[2] Gene set enrichment analysis (GSEA) was done to compare the androgen-repressed genes in C4-2-tet-shRB versus VCaP/VCaP-CR cells. NES, normalized enrichment score. (B) Enrichments of HALLMARK_E2F_TARGETS and HALLMARK_MYC_TARGET_V1 gene sets were plotted. (C) GSEA was done to compare directly androgen-repressed genes (AR-repressed genes with nearby AR binding) in these cells. (D–G) ChIP-seq analyses were performed in C4-2 cells treated with ethanol or DHT (10 nM, 4 h). Venn diagrams (D and E) or heatmap view (F and G) for Rb or c-Myc binding peaks were shown. (H) Binding and expression target analysis (BETA) for the association of Rb or c-Myc binding sites (DHT stimulated) with the expression of AR-repressed genes identified from RNA-seq (A). n.s., not significant.

S3C–S3E and Table S1, E2F target genes were broadly repressed by DHT, but this repression effect was significantly attenuated by Rb silencing. Many *E2F* family genes, particularly activator E2Fs (E2F1–3), are known as direct targets of Rb-E2F repressor complex,[40] and their expression was also AR repressed and mediated by Rb (Figure 2E). One major activity of Rb-E2F complex is to suppress DNA synthesis via transcriptional repression of MCM helicase and other DNA replication factors.[41] A group of these genes (77 genes) was previously identified as AR-repressed genes,[5] and the full repression activity of DHT on these genes was also dependent on Rb expression (Figure S3F). On the contrary, *MYC*, *PCAT-1* (function to stabilize c-Myc protein),[42] and many Myc target genes were repressed by androgen treatment, but this repression effect was not significantly affected by Rb depletion (Figures 2D, lower panel, and 2F).

Since increased E2F expression is a result of Rb depletion, we next examined whether the impairment of AR-mediated repression is directly due to the elevated expression of E2Fs. To test this hypothesis, we stably expressed a doxycycline-inducible E2F1 in C4-2 cells (Figure S4A). Interestingly, overexpression of E2F1 modestly enhanced AR binding to the activation sites and the DHT-induced expression of AR-activated genes (Figures S4B and S4C). However, the AR binding to the suppression sites and DHT-induced repression of DNA-replication genes were not affected (Figures S4D and S4E), suggesting that overexpression of E2F is not sufficient to impair the transcriptional repression activity of AR on DNA synthesis and cell cycle genes. The epigenetic modifier EZH2 was also shown to be a critical target of Rb-E2F, and *RB1* loss can induce EZH2 activity in neuroendocrine PCa.[24,25,43] Since EZH2 was reported to involve in the transcriptional repression activity of AR,[3] we next examined whether EZH2 inhibition can impair the AR-mediated repression on DNA synthesis and cell cycle genes. As shown in Figure S5, treating C4-2 cells with an EZH2-specific inhibitor (GSK126) modestly decreased the basal expression of DNA synthesis genes but did not appear to significantly alter the DHT-induced transcriptional repression on these genes, indicating that EZH2 is not involved in this specific activity of AR.

To further confirm the Rb dependence in androgen-induced transcriptional repression of DNA synthesis and cell cycle, we also generated *RB1* knockout (RB-KO) stable clones using the CRISPR-Cas9 approach (Figure 2G). These RB-KO clones developed resistance to enzalutamide treatment (Figure 2H), consistent with previous findings.[25,27] Importantly, the androgen-induced cell cycle repression was significantly impaired in RB-KO cells (Figure 2I). A similar effect

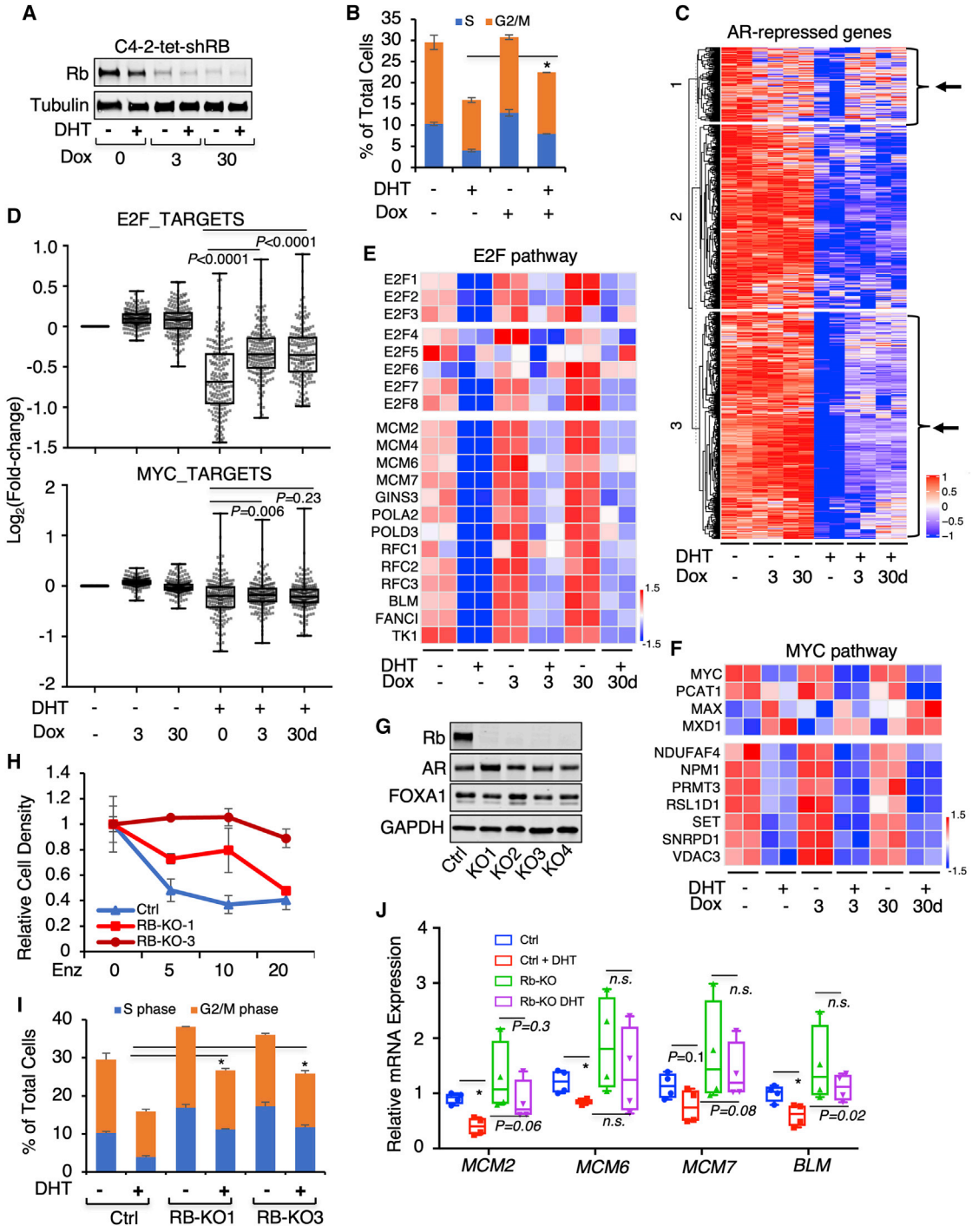

Figure 2. Rb depletion compromises global AR repression activity

(A) Immunoblotting for Rb in C4-2-tet-shRB cells treated with doxycycline (0.05 μg/mL) at 0, 3, or 30 d (days). (B) The flow cytometry cell cycle analysis for C4-2-tet-shRB cells treated with or without doxycycline and with or without 10 nM DHT for 24 h. (C) RNA-seq analyses were done in C4-2-tet-shRB cells treated with doxycycline (0.05 μg/mL at 0, 3, or 30 days) and stimulated with or without DHT (10 nM, 24 h). Heatmap view for DHT-repressed genes was shown. (D) Box plots for the change of expression (Log_2(fold-change)) for E2F target genes or Myc target genes in these samples are shown. (E) Heatmap view for *E2Fs* (upper panel) and a panel of E2F target genes (lower panel) is

(legend continued on next page)

was also observed when examining the androgen-induced repression of several DNA synthesis genes (although clonal variation was observed; Figure 2J), confirming the critical role of Rb in mediating the transcriptional repression activity of AR. Overall, these *in vitro* studies clearly demonstrated a critical role of Rb in mediating the transcriptional repression and tumor-suppressive activities of high-dose androgens in CRPC.

p130 compensates for the absence of Rb in mediating the transcriptional repression activity of AR in Rb-depleted cells

Since Rb depletion cannot completely prevent the androgen-mediated transcriptional repression of E2F signaling (see Figure 2D), it suggests that additional factors may be involved in mediating E2F activity when Rb expression level is low or absent. One possible factor is ZBTB7A, which can act as a corepressor of AR and mediate AR transcriptional repression of E2F signaling.[6] Other factors may include Rb-like pocket proteins, p107 and p130 (encoded by *RBL1* and *RBL2*, respectively), which were known to form complex with E2Fs (such as DREAM complex)[44] and play an important role in regulating E2F signaling. It is also known that these pocket proteins (Rb/p107/p130) have partly redundant activities and can often compensate for each other if one is inactivated or absent. In addition, p130 has been shown to regulate the AR-mediated repression of EZH2 in PCa cells.[14,45] While *RBL1* expression was generally low in CRPC patient samples (SU2C metastatic CRPC dataset),[23] *RBL2* expression was much higher in CRPC. Moreover, *RBL2* deep deletions were detected in ~3.5% of CRPC samples (SU2C, analyzed through cBioPortal)[46,47] and appear to be mutually exclusive to *RB1* deletion (Figure S6A), suggesting *RBL2* may play a similar tumor suppressor function in CRPC progression. Therefore, we next focused on examining whether *RBL2*/p130 is involved in mediating the transcriptional repression activity of AR.

We first examined the chromatin binding of p130 in C4-2-tet-shRB cells using ChIP-seq analyses. In the untreated cells, the majority of Rb-binding sites (~80%) and E2F1-binding sites[28] (~60%) were overlapped with p130 binding (~25% and ~70% of its total binding sites, respectively; Figures 3A and 3B), suggesting that p130 may function alternatively to Rb to form complexes with E2Fs. Examining several previously identified Rb-binding sites, we confirmed the occupancy of p130, which can be similarly enhanced by the androgen treatment (Figure S6B). Interestingly, the total number of p130 binding peaks was decreased when Rb expression was silenced, but the remaining p130 peaks showed increased overlapping with E2F1 binding (~80% of p130 peaks) and were strongly associated with Rb-E2F-repressed genes (Figures 3C, 3D, and S6C). Moreover, the interaction between p130 and E2F1 was markedly increased by Rb depletion and can be further strengthened by a CDK4/6 inhibitor, palbociclib, which blocked the phosphorylation of p130 (Figures 3E–3G), suggesting that p130 may be similarly regulated by CDKs and function to compensate for the loss of Rb to repress the activity of E2Fs.

Next, we determined whether p130 contributes to the transcriptional repression activity of AR in Rb-depleted cells. The *RBL2* mRNA expression was slightly decreased by Rb ablation (Figure S6D), but its protein expression was barely affected (see Figure 3E). Notably, the chromatin binding of p130 was significantly associated with AR repression function when Rb expression was silenced (Figure 3H). Interestingly, knocking down *RBL2* also decreased Rb protein and mRNA expression (Figures 3I and S6E), indicating an additional function of *RBL2* to support *RB1* expression in C4-2 cells. Nonetheless, co-silencing both *RB1* and *RBL2* further blocked the repression activity of DHT on E2F-regulated DNA replication genes and the cell cycle progression (Figures 3J and 3K). Similar results were also obtained from co-silencing *RB1* and *RBL2* in VCaP model (Figures S7A and S7B). Together, these data indicate that p130 participates in the androgen-induced transcriptional repression of E2F signaling and may partially compensate for the absence of Rb.

Rb depletion alters AR chromatin binding

While our data indicated that Rb depletion may broadly compromise the androgen-induced repression of genes, it is unclear whether Rb is important to maintain AR chromatin binding. To determine this, we carried out AR ChIP-seq in C4-2-tet-shRB cells treated with or without doxycycline and stimulated by high-dose androgens (10 nM DHT) to identify AR binding sites. As shown in Figures 4A and 4B, DHT treatment markedly increased AR chromatin binding in both doxycycline-treated (3 d) and untreated cells. However, the DHT-induced AR binding sites were significantly altered in Rb-depleted cells versus the control cells (Figure 4C), indicating a rapid redistribution of AR chromatin binding by Rb inactivation. We then performed ChIP-seq of FOXA1, a critical pioneer factor of AR,[48,49] to determine whether Rb depletion can affect FOXA1 chromatin binding prior to AR recruitment. To minimize the feedback effect of AR on FOXA1 chromatin binding,[50] we carried out this experiment in the absence of DHT. Interestingly, unlike the massive redistribution of AR binding, the FOXA1 binding sites were largely conserved in Rb-depleted cells (Figure 4D), indicating that Rb depletion did not alter FOXA1 binding. Significantly, ~70% of AR binding sites (13,256) were lost by Rb depletion, and these "lost" sites had weaker AR binding than the "conserved" sites but were strongly associated with AR and FOXA1 binding motifs (Figures 4E and 4F). Moreover, ~30% (223/806) of AR-repressed genes contained at least one of these "lost" sites and the repression of these genes was impaired

shown. (F) Heatmap view for *MYC* and its coregulators (upper panel) and a panel of Myc target genes (lower panel) is shown. (G) Immunoblotting for Rb, AR, and FOXA1 in control C4-2 cells versus selected clones of C4-2 with *RB1* knockout (KO1–4) using CRISPR-Cas9 approach is shown. (H) The proliferation assay for control C4-2 cells and two RB-KO lines treated with 0–20 μM of enzalutamide for 6 d is shown. (I) The flow cytometry cell cycle analysis for the control C4-2 and two RB-KO clones is shown. (J) Quantitative real-time PCR for several E2F-regulated genes in control lines versus RB-KO lines is shown. Data in bar graphs represent the mean ± SD. n.s., not significant. *$p < 0.05$.

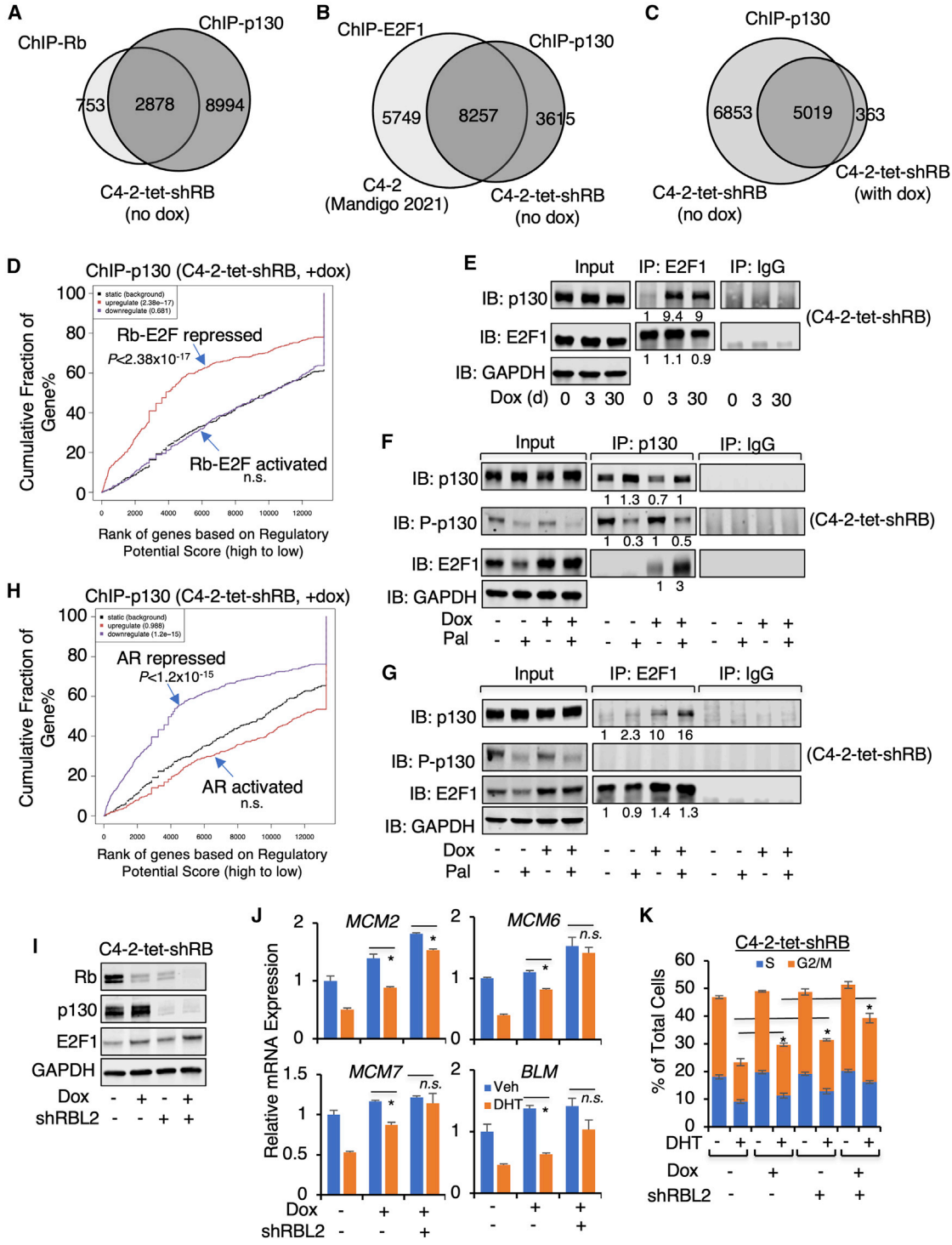

Figure 3. p130 compensates for the absence of Rb in mediating the transcriptional repression activity of AR

(A and B) ChIP-seq analysis of p130 was performed in uninduced C4-2-tet-shRB cells (no doxycycline). The Venn diagram for p130 and Rb (A) or p130 and E2F1 (B) overlapping binding peaks was shown. (C) ChIP-seq analysis of p130 was performed in C4-2-tet-shRB cells treated with vehicle or doxycycline (3 d). The Venn diagram for p130 binding peaks in both conditions was shown. (D) BETA for the association of p130 binding peaks (doxycycline treated) with the expression of Rb-repressed genes identified from RNA-seq of C4-2-tet-shRB (doxycycline versus vehicle) is shown. (E) Immunoprecipitation (IP) of E2F1 in C4-2-tet-shRB cells (doxycycline for 0, 3, or 30 d), followed by immunoblotting for p130 or E2F1, is shown. (F and G) IP of p130 (F) or E2F1 (G) in C4-2-tet-shRB cells cultured with or without doxycycline and treated with

(legend continued on next page)

by Rb depletion (Figures 4G and 4H), suggesting that Rb depletion may disrupt AR chromatin binding at a subset of suppressive androgen response elements (AREs). On the contrary, AR-activated genes containing lost sites did not seem to be affected by Rb depletion (Figures S8A and S8B).

Rb depletion also resulted in 13,189 "gained" AR sites, but these sites were not occupied by FOXA1 or enriched for AR/FOXA1 binding motifs. Indeed, the gained AR binding sites appeared to contain binding motifs for a distinct set of transcription factors, including zinc finger and BTB-domain-containing proteins (ZBTB3), nuclear receptor family members (HNF4A and VDR), glial cells missing transcription factors (GCM1), nescient helix loop helix 1 (NHLH1), and E2Fs. We next conducted a combined analysis using these ChIP-seq data and RNA-seq data from C4-2-tet-shRB cells to identify genes that were associated with gained AR chromatin binding and AR regulation upon Rb depletion. This analysis resulted in the identification of 41 new androgen-repressed genes but only 24 new androgen-induced genes (Figure 4I). While we did not find any pathway enrichment in the androgen-induced genes, these new androgen-repressed genes were enriched in the pathways of maintaining cell polarity (Figure 4J), which may contribute to cancer progression and regulation of cell lineage plasticity. These genes include *FRMD4B*, *MARK1*, and *FGF13* (Figure 4K), and the expression of cytoplasmic FGF13 protein has been previously reported to correlate with increased risk of biochemical recurrence of PCa.[51] Overall, these results indicate that Rb expression is critical for maintaining AR chromatin binding and that Rb depletion can disrupt canonical AR binding at a subset of AR-repressed gene loci and may also promote noncanonical AR binding to repress a set of new targets.

Rb depletion desensitizes CRPC responses to high-dose androgen treatment

Deletion of *RB1* is commonly found in CRPC and contributes to its progression.[23] While the above results clearly indicated a central role of Rb family proteins in mediating the global repression activity of AR, it is not clear whether CRPC tumors with *RB1* loss may completely turn into non-responders to high-T treatment. Therefore, we next sought to determine whether Rb activity affects the tumor response to high-T treatment *in vivo*. Xenograft tumors derived from C4-2-tet-shRB cells were established in castrated male severe combined immunodeficiency (SCID) mice, and *RB1* silencing was induced by switching the regular diet to a doxycycline-supplemented diet (Figure S9A). These mice were then treated with two doses of testosterone treatments, both of which were well tolerated by the animals (Figures S9B and S9C). The lower dose of testosterone treatment (40 mg/kg) that was used in the experiment is comparable with the dose used in the previous preclinical studies and clinical trials.[8-10] The growth of Rb-proficient C4-2 tumors was markedly repressed by both testosterone treatments (Figure 5A). However, while the higher dose of testosterone (160 mg/kg) can still suppress the growth of Rb-deficient tumors, the lower dose of testosterone treatment showed a reduced efficacy in treating these tumors (Figure 5B). To further confirm this finding, we also selected an RB-KO clone (Figure 5C) to determine the effect of *RB1* loss on the tumor-suppressive effect of DHT. While 10, 100, or 1,000 nM DHT treatment can similarly repress C4-2 cell proliferation, *RB1* loss appeared to have a stronger effect on the lower doses of DHT versus higher doses of DHT (Figure 5D). We then generated xenograft tumors using this RB-KO line and similarly treated mice with two doses of testosterone. As shown in Figure 5E, the RB-KO tumor did not respond to the lower dose of testosterone but modestly responded to the higher dose. This result is consistent with the observation in the C4-2-tet-shRB model, but the tumor-suppressive effect of high-T appeared to be more significantly impaired by the complete silencing of *RB1*.

We next performed an RNA-seq analysis in the tumor samples from C4-2-tet-shRB xenografts to determine the impact of high-T (higher dose) on tumor cell transcriptomes (Figures 6A and S10A). The androgen-repressed genes were significantly enriched for E2F signaling, cell cycle pathways (G2M checkpoint and mitotic spindle), and NE-up genes in Rb-proficient tumors but were noticeably less enriched for these pathways in Rb-depleted tumors, despite that the tumor growth was still repressed by this dose of high-T. In contrast, the enrichment of Myc signaling (MYC_TARGET_V1) and DNA repair pathway were not significantly affected by Rb silencing, indicating a persistent repression activity on these pathways. Interestingly, we have also observed the enrichment of the oxidative phosphorylation pathway in both conditions, which was not seen in the cell line studies. Moreover, the high-T treatment specifically repressed p53 and protein secretion pathways in Rb-silenced cells. The androgen-mediated repression of the *AR* gene itself was not affected by Rb depletion (Figure S10B). As expected, high-T upregulated genes were enriched for the androgen response pathway and the enrichment was not significantly affected by Rb depletion (see Figure S10A).

Next, we compared the androgen-repressed expression of E2F signaling targets versus Myc signaling targets in these tumor samples. As shown in Figures 6B–6D and S10C–S10E, the E2F signaling was strongly repressed by the high-T treatment, but this repression effect was significantly compromised by Rb depletion. On the contrary, the repression on Myc signaling was much weaker than E2F signaling, and it was clearly less affected by Rb depletion, suggesting that sustained repression on Myc signaling may contribute to the effectiveness of high-T treatment (with increased dose) on Rb-deficient tumors. We next examined whether Rb-depletion-induced reprogramming of AR could contribute to the tumor-suppressive effect of

vehicle or palbociclib (1 μM, 24 h), followed by immunoblotting for total p130, p-p130 (S672 phosphorylated), or E2F1 is shown. (H) BETA for the association of p130 binding peaks (doxycycline treated) with the expression of AR-repressed genes identified from RNA-seq of C4-2-tet-shRB (doxycycline treated) is shown. (I–K) C4-2-tet-shRB cells stably infected by lentiviral shRNAs against NTC or *RBL2* were treated with vehicle or doxycycline (6 d), followed by immunoblotting for Rb, p130, and E2F1 (I), quantitative real-time PCR for E2F-regulated genes (J), and the flow cytometry cell cycle analysis (K). Data in bar graphs represent the mean ± SD. n.s., not significant. *$p < 0.05$.

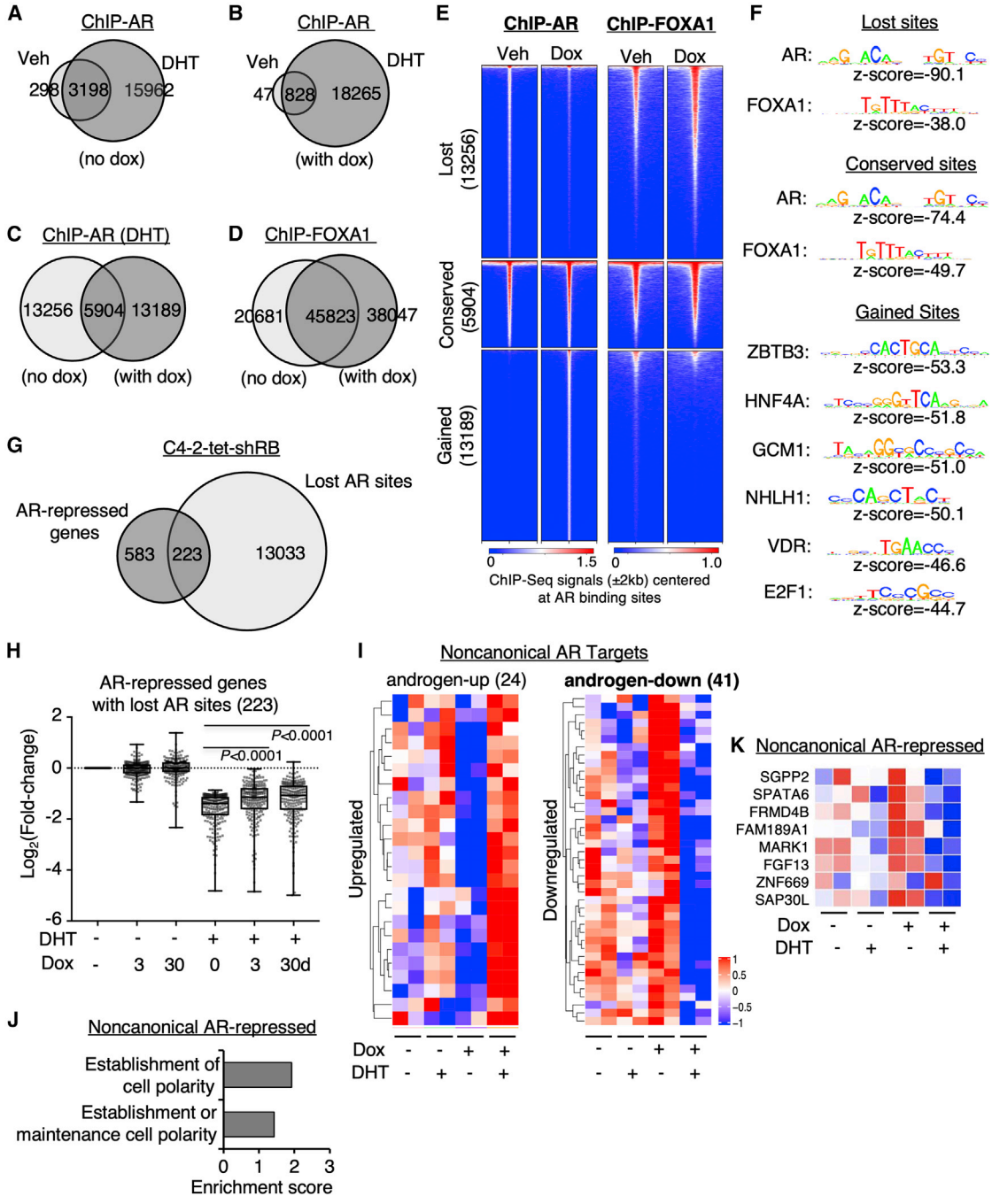

Figure 4. Rb depletion reprograms the transcriptional repression activity of AR

(A–C) ChIP-seq analyses of AR were performed in C4-2-tet-shRB cells cultured with vehicle or doxycycline (3 days) and then stimulated with ethanol or DHT (10 nM, 4 h). Venn diagrams for AR binding peaks in cells treated with DHT versus ethanol in the absence of doxycycline (A), DHT versus ethanol in the presence of doxycycline (B), and doxycycline versus vehicle in the presence of DHT (C) were shown. (D) ChIP-seq analyses of FOXA1 were performed in C4-2-tet-shRB cells cultured with vehicle or doxycycline. The Venn diagram for FOXA1 binding peaks in both conditions was shown. (E) Heatmap view for ChIP-seq signal intensity of AR and FOXA1 at clustered AR-binding sites (lost, conserved, and gained) is shown. (F) Motif enrichment analysis for these AR binding sites is shown. (G) The Venn diagram for AR-repressed genes and the gene annotation of the "lost" AR sites is shown. (H) Box plots for the change of expression of AR-repressed genes containing at least one lost AR site in C4-2-tet-shRB cells are shown. (I) Heatmap view for *RB1*-silencing-induced AR-reprogramming targets determined by gained AR binding and regulation (fold-change > 1.5) is shown. (J) Gene ontology analyses for the reprogrammed AR-repressed genes are shown. (K) Heatmap view for a panel of reprogrammed AR-repressed genes is shown.

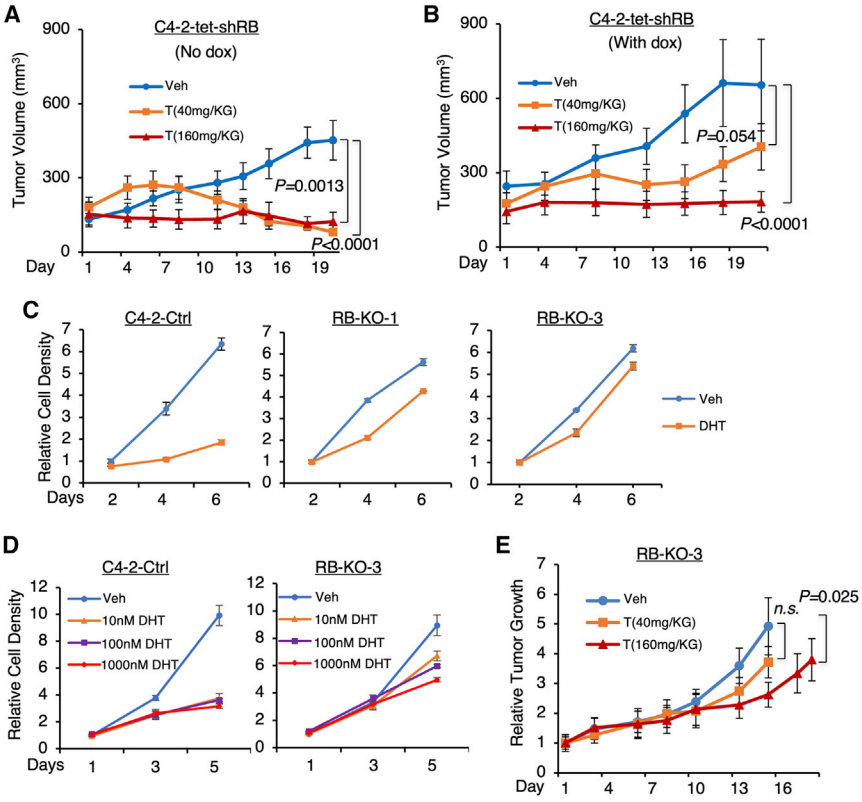

Figure 5. Rb depletion desensitizes CRPC tumor response to high-T

(A and B) Xenograft tumors derived from C4-2-tet-shRB cells were established in castrated male SCID mice. Tumor-bearing mice fed with a regular diet (A) or a doxycycline-supplemented diet (B) were daily injected with vehicle or testosterone (40 mg/kg or 160 mg/kg). Tumor volume was measured manually by caliber (n = 6). Note: the two xenograft experiments were done independently. (C) Cell proliferation assay for control C4-2 cell line and two RB-KO cell lines treated with or without DHT (10 nM, 0–6 d) is shown. (D) Cell proliferation assay for control C4-2 cell line and RB-KO-3 cell line treated with or without DHT (0–1,000 nM, 0–5 d) is shown. (E) Xenograft tumors derived from RB-KO-3 line were established in castrated male SCID mice. Tumor-bearing mice were then daily injected with vehicle or testosterone (40 mg/kg or 160 mg/kg). Tumor volume was measured manually by caliber (n = 4). Data in growth curves represent the mean ± SE. n.s., not significant.

high-T. Indeed, many noncanonical AR repression targets, including the identified cell polarity genes, were repressed in Rb-deficient tumors, but not in Rb-proficient tumors (Figure 6E). Together, these results suggest that *RB1*-loss CRPC is less sensitive to the high-T treatment but may still respond to higher doses of testosterone treatments (super high-T), possibly through mediating multiple Rb-independent mechanisms.

CDK4/6 inhibition enhances the efficacy of high-T treatment in CRPC models

CDK4/6 inhibitor treatment has been approved in treating ER-positive and HER2-negative breast cancer[52] but appears to be less effective in the clinical trials of prostate cancer.[53] One major downstream effect of CDK4/6 inhibition is to block the hyperphosphorylation of Rb, which disrupts the Rb-E2F repressor complex. In addition, Rb-like proteins were also previously demonstrated as the direct targets of CDK4/6. Therefore, we first examined whether palbociclib, a US Food and Drug Administration (FDA)-approved CDK4/6 inhibitor,[54,55] can prevent the hyperphosphorylation of Rb and p130 in CRPC cells. In C4-2-tet-shRB cells, palbociclib treatment markedly repressed the phosphorylation of Rb and p130 in the absence or presence of androgen treatments (Figure 7A), indicating that CDK4/6 inhibition can effectively target Rb/p130-E2F complex. We next determined whether CDK4/6 inhibition can be used to improve high-T treatment in CRPC cell lines. As seen in Figures 7B and 7C, palbociclib treatment clearly enhanced the transcriptional repression effect of DHT on DNA synthesis genes and the suppression effect on cell cycle progression.

Since Rb depletion altered AR chromatin binding (see Figure 4), we next determined whether Rb enhancement by CDK4/6 inhibition can also redistribute AR binding in C4-2 cells. Using ChIP-seq analysis of AR in C4-2 cells treated with DHT and palbociclib, we identified 9,974 high-confidence AR-binding peaks. This distinct AR-binding program had very limited overlapping sites with AR bindings in Rb-proficient C4-2 cells (1,707 sites) or Rb-depleted cells (1,528 sites; Figure S11A). We then performed a motif enrichment analysis for the lost, conserved, and gained AR sites in comparison with the regular AR-binding program (Figure S11B). While the lost and the conserved AR-binding sites contained classic AREs, the gained AR-binding sites have no enrichment of known AR-binding sequences. Instead, AR appeared to bind to sites that contain E2F or altered E2F-binding nucleotide sequences (Figure S11C). Moreover, examining a panel of gene loci with gained AR binding, we also found that the gained AR-binding sites appeared to be also co-occupied by Rb (Figure S11D). These data strongly suggest that CDK4/6 inhibition may redistribute AR binding to the sites that are occupied by Rb-E2F repressor complex.

To test the efficacy of the combination treatment *in vivo*, we passaged a series of LuCaP CRPC PDX models in castrated SCID mice, including 35CR, 70CR, 77CR, and 96CR. While all four models have *AR* gene amplification, 35CR is $RB1^{+/+}$, 70CR and 77CR are $RB1^{+/-}$, and 96CR is $RB1^{-/-}$.[56] Using the reported RNA-seq data generated from these models,[8] we showed that the expression levels of *RB1* and *RBL2* were higher in 35CR and lower in LuCaP96CR (Figure 7D). These results were also validated by ChIP-qPCR using tumor RNA samples (Figure S12A). Since *RB1* copy-number change and mRNA expression may not fully reflect the deficiency of Rb, we

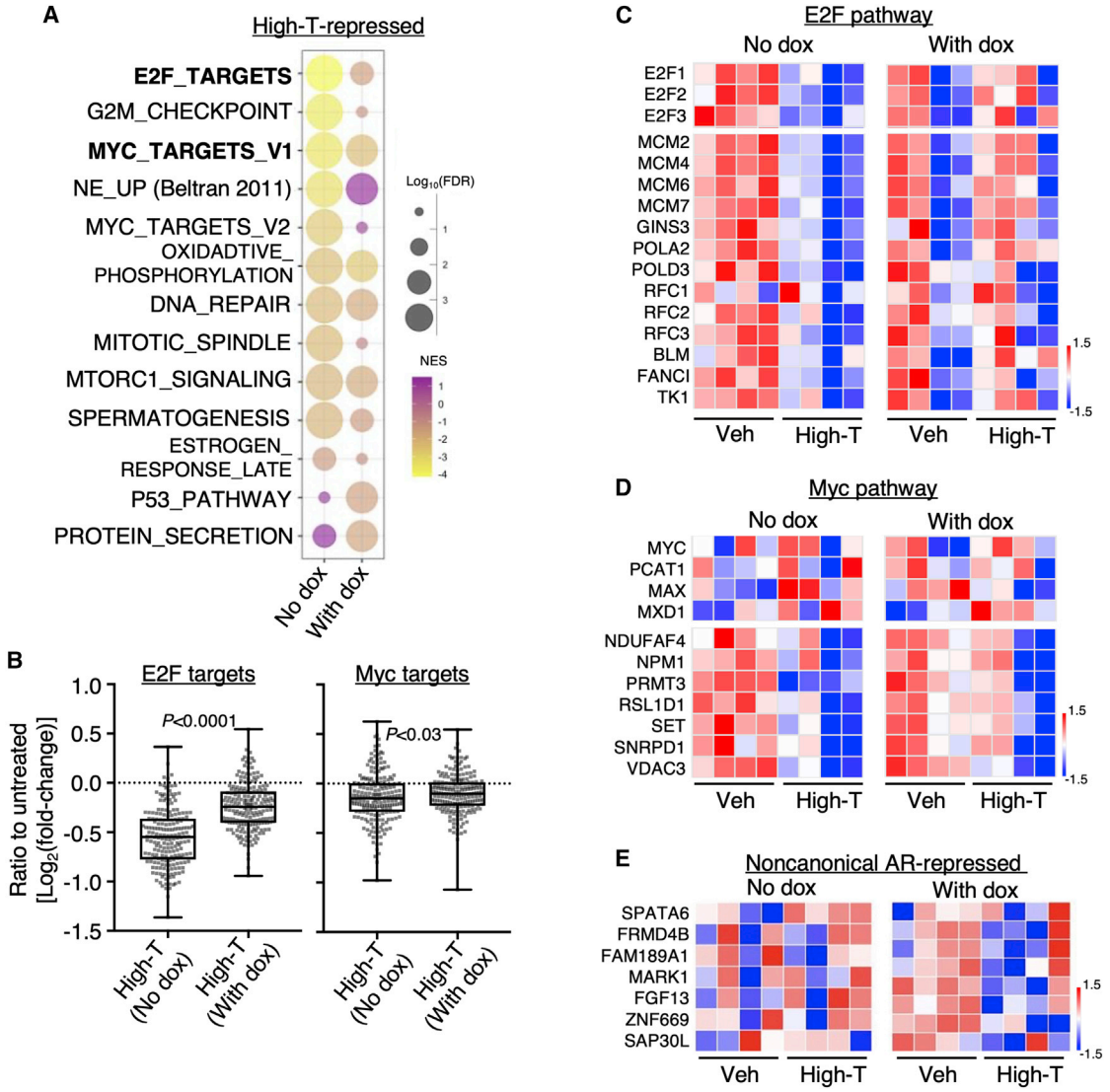

Figure 6. Rb depletion impairs high-T-induced transcriptional repression on E2F signaling

(A) RNA-seq analyses were performed using tumor samples (treated with 160 mg/kg testosterone) at the end of the experiments. GSEA was done to compare the androgen-repressed genes in Rb-proficient tumors versus Rb-deficient tumors. (B) Box plots for the change of expression (Log_2(fold-change)) for E2F target genes or Myc target genes in these samples are shown. (C) Heatmap view for E2Fs (upper panel) and a panel of E2F target genes (lower panel) is shown. (D) Heatmap view for *MYC* and its coregulator genes (upper panel) and a panel of Myc target genes (lower panel) is shown. (E) Heatmap view for a panel of noncanonical AR-repressed genes is shown.

next assessed the Rb activity in these models using a recently developed gene signature of Rb directly repressed targets.[57] Surprisingly, the score of Rb targets in 70CR tumors appeared to be much higher than other models (Figure 7E), suggesting that Rb may be inactivated in this model due to other mechanisms. Interestingly, we also consistently detected Rb mRNA expression in the 96CR model (comparable to the expression level in C4-2) despite that it was previously reported as an *RB1*-loss model.[56] Indeed, the phosphorylated Rb proteins were detected in 96CR tumor samples (Figure S12B), suggesting that 96CR tumors may be heterogeneous and still contain a significant portion of Rb-positive cells. All four models expressed comparable or higher levels of AR in comparison with C4-2 CRPC xenograft tumors (Figures S12C and S12D).

We next treated all these PDX models with the combination treatment. As shown in Figures 7F–7H, the high-T treatment alone significantly repressed the tumor growth in Rb-proficient models, including 35CR, 77CR, and 96CR, consistent with previous findings.[8] While palbociclib treatment alone repressed tumor growth in 35CR and 77CR, but not 96CR, the enhanced tumor-suppression effect in combination with high-T was observed in all these three responders. On the contrary, the possible Rb-deficient 70CR tumors showed no

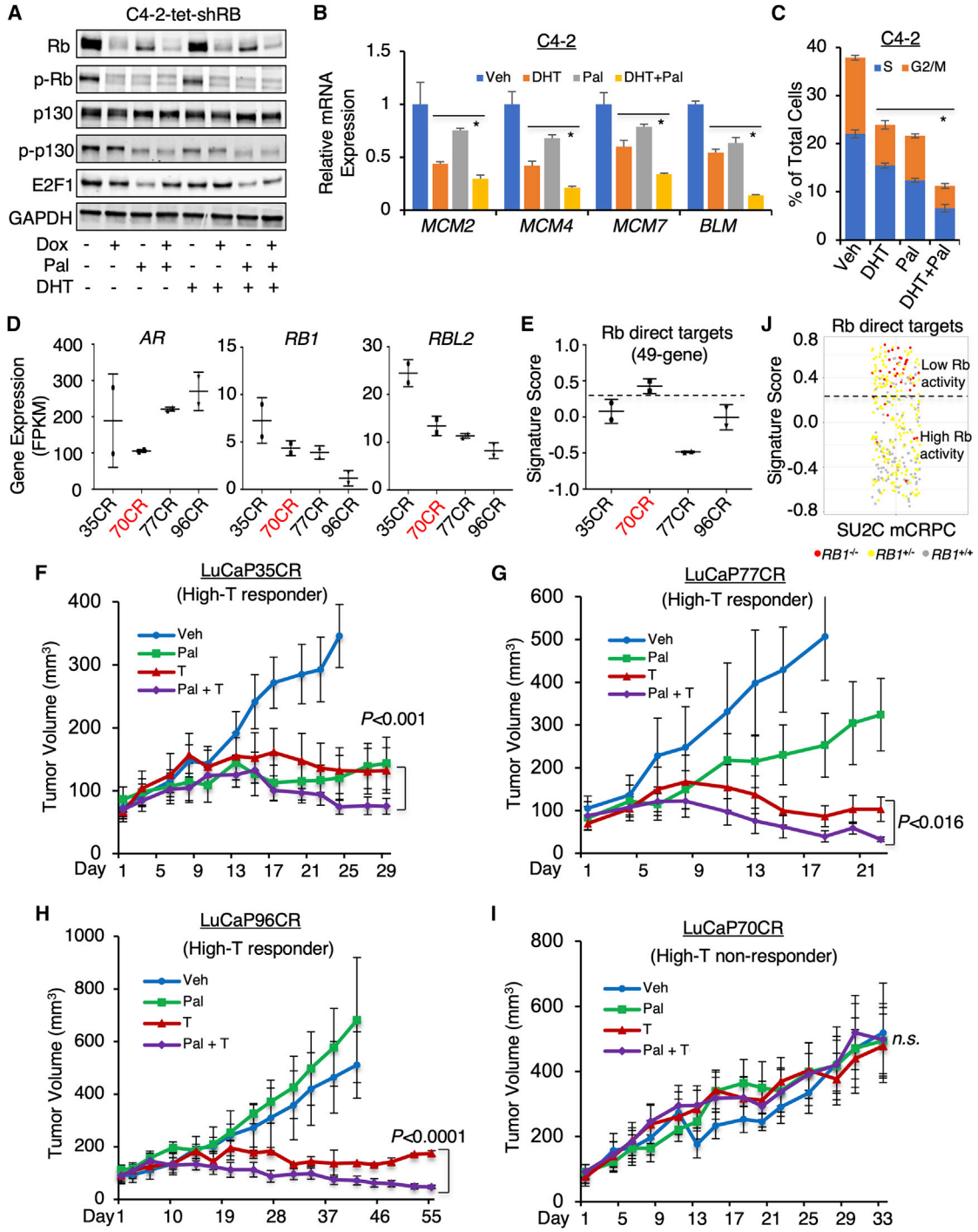

Figure 7. CDK4/6 inhibition enhances the growth-suppressive activity of high-T in CRPC

(A) Immunoblotting for total Rb, p-Rb (S780 phosphorylated), total p130, p-p130 (S672 phosphorylated), and E2F1 in C4-2-tet-shRB cells treated with vehicle, doxycycline (3 d), palbociclib (1 μM), or DHT (10 nM) for 24 h. (B and C) Quantitative real-time PCR for the expression of E2F-regulated genes (B) or flow cytometry cell cycle analysis (C) in C4-2 cells treated with DHT (10 nM, 24 h), palbociclib (1 μM, 24 h), or the combination is shown. (D) mRNA expression (from RNA-seq) for *AR*, *RB1*, and *RBL2* in tumor samples from LuCaP PDXs is shown. (E) Signature scores of Rb-target genes (directly repressed) in tumor samples from LuCaP PDXs are shown. (F–I) Castrated SCID male

(legend continued on next page)

response to high-T or the combination treatment (Figure 7I). These data suggest that the repressor activity of Rb may be a critical molecular determinant for the efficacy of high-T and the combination treatment in CRPC patients. Applying the Rb-target signature in the public mCRPC patient dataset (SU2C mCRPC),[23] we can then separate tumors with lower Rb activity (higher scores) versus higher Rb activity (lower scores) and predict that the tumors with high Rb activity may respond better to the high-T and the combination treatments (Figure 7J).

We next conducted an RNA-seq analysis using tumor samples from the LuCaP35CR study. The inhibition of Rb phosphorylation by palbociclib was confirmed by immunohistochemistry staining (Figure S13A). While 1,220 genes or 1,403 genes were downregulated by high-T or palbociclib treatment, respectively, significantly more genes (2,750) were repressed by the combination treatment (Figure 8A). The combination treatment also showed a much stronger repression effect on these genes than any single-agent treatment (Figure 8B). Using gene set enrichment analysis (GSEA), we found that the downregulated genes by the single or combination treatment were enriched for E2F signaling, Myc signaling, cell cycle regulation, and DNA damage repair pathway, while the upregulated genes were enriched for androgen response and apoptosis (Figures 8C and S13B–S13D). We next examined the effects of those treatments on E2F and Myc signaling genes. As shown in Figure 8D, both pathways were repressed by either high-T or palbociclib treatment, and the repression effect was further enhanced by the combination treatment. However, the repression effect on E2F pathway genes appeared to be stronger than the effect on Myc pathway genes, consistent with the *in vitro* study that showed higher repression activity of AR on E2F target genes. This enhancing effect was also seen from a panel of E2F or Myc target genes (Figures 8E and 8F). On the contrary, the *AR* gene was repressed only by high-T, but not palbociclib, and no additive effect was observed (Figure S13E). Furthermore, we also examined how redistributed AR binding induced by CDK4/6 inhibition may affect gene expression regulated by the combination treatment. By comparing the RNA-seq data from combination treatment versus high-T alone and using AR ChIP-seq in C4-2 model treated with DHT and palbociclib, we found 1,159 upregulated genes and 832 downregulated that were associated with nearby AR-binding sites (Figure S14A). Importantly, while the upregulated genes were only enriched for tumor necrosis factor alpha (TNFα) pathway, the downregulated genes were highly enriched for E2F targets, NE_up genes, and cell cycle genes, but not Myc targets (Figure S14B), suggesting that the CDK4/6-inhibition-induced alteration of AR binding may contribute to the overall combinatory effect of palbociclib and testosterone. Together, these data highly suggest that the high-T treatment can be combined with CDK4/6 inhibitors to treat patients with AR-positive and Rb/p130-proficient CRPC.

DISCUSSION

Rb is a transcriptional repression partner of E2Fs, and Rb-E2F repressor complex is critical for cells to repress DNA synthesis and other events prior to cell cycle transition from G1 to S phase.[20] Hyperphosphorylation of Rb by cyclin D-CDK4/6 and cyclin E-CDK2 disrupts the Rb-E2F complex and leads to the transcriptional activation of E2Fs.[58] A previous study has identified an androgen-induced AR-Rb interaction at chromatin that promotes the activity of Rb-E2F repressor complex. Therefore, in this study, we attempted to determine whether this activity of AR is a primary mechanism for the anti-tumor activity of high-dose androgens. We performed a series of global studies and demonstrated that E2F signaling is the major direct downstream target of the transcriptional repression function of AR induced by high-dose androgen treatment, which is mediated through increased global chromatin binding of the Rb-E2F complex (see Figure 1). Furthermore, we determined that Rb activity is important for the CRPC sensitivity to high-dose androgen treatments *in vitro* and *in vivo*. Mechanistically, we also demonstrated that an Rb-like pocket protein, p130, was similarly involved in this activity by interacting with E2Fs particularly when Rb expression is low. While we did not examine the requirement of p130 for the high-T treatment *in vivo*, we predict that depleting p130 expression would also desensitize CRPC tumor to high-T. Future studies are clearly needed to demonstrate the *in vivo* role of p130 in the presence or absence of Rb using CRPC xenograft models. Importantly, our finding is also consistent with a recent study using a series of castration-resistant LuCaP PDX models, which demonstrated that the most robust molecular phenotype for high-T treatment is the suppression of E2F transcriptional output.[8]

RB1 loss is common in CRPC, and this event causes profound genomic consequences. In this study, we show that *RB1* loss may also reshape AR cistrome by broadly disrupting AR binding from canonical AREs and redistributing AR chromatin binding to low-affinity noncanonical sites lacking classic FOXA1- and AR-binding motifs (see Figure 4). These new AR-binding sites appeared to be enriched for the binding motif of ZBTB family proteins, and our recent study indicates that ZBTB7A can function as a corepressor of AR to directly mediate its transcriptional repression activity.[6] Therefore, the reprogrammed sites may favor the interaction of AR and ZBTB7A to repress a distinct subset of genes. Indeed, this redistribution of AR appeared to have a stronger impact on reprogramming AR transcriptional repression activity than activation activity, and we have identified a large set of canonical AR-repressed genes with reduced AR-repression activity and a small set of genes that may gain AR-mediated repression in Rb-depleted cells. Interestingly, these noncanonical targets enriched for pathways of maintaining cell polarity and deregulation of cell polarity proteins have been known to be crucial for cancer progression, including lineage plasticity.[59,60] One of the new AR-repressed genes is a member of fibroblast growth factor (FGF)

mice bearing LuCaP35CR (F), 77CR (G), 96CR (H), and 70CR (I) xenograft tumors were daily treated with vehicle, testosterone (40 mg/kg), palbociclib (150 mg/kg), or the combination via intraperitoneal injection (for high-T) or oral gavage (for palbociclib; n = 6). Tumor volume was measured by caliper. (J) Signature scores of Rb-target genes (directly repressed) in SU2C mCRPC dataset are shown. Data in bar graphs represent the mean ± SD. Data in growth curves represent the mean ± SE. n.s., not significant. *,$p < 0.05$.

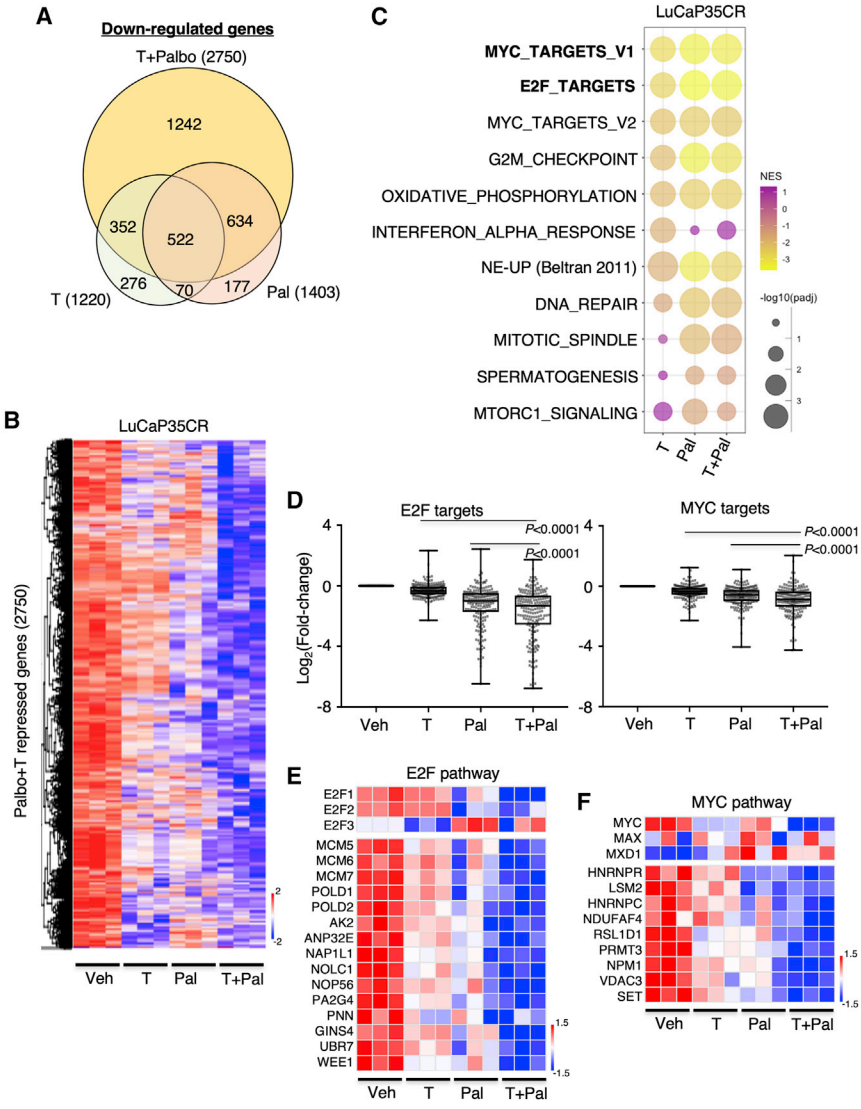

Figure 8. Gene profiling in LuCaP35CR tumors receiving the combination treatment

(A) RNA-seq analyses were performed using tumor samples from the LuCaP35CR study (at the end of the experiment). The Venn diagram for high-T-repressed genes, palbociclib-repressed genes, and the combination treatment-repressed genes is shown. (B) Heatmap view for the combination treatment-repressed genes in all tumor samples is shown. (C) GSEA for the downregulated genes by single treatments versus the combination treatment is shown. (D) Box plots for the change of expression of E2F target genes or Myc target genes in these samples are shown. (E and F) Heatmap view for E2Fs and E2F target genes (E) or *MYC* and its coregulator genes and a panel of Myc target genes (F) is shown.

homologous factors, *FGF13*, which has been shown to associate with poor patient outcomes in PCa[51] and promotes the metastasis of triple-negative breast cancer.[61] Interestingly, FGF signaling has been also shown to drive PCa progression in double-negative (AR-negative and NE-null) CRPC.[62] Therefore, possibly suppressing FGF signaling by high-T may represent a novel tumor-suppressor activity of AR to prevent lineage plasticity and cancer progression in *RB1*-loss CRPC. Nonetheless, the biological significance of this noncanonical AR repression activity in Rb-deficient cells remains to be determined in future studies. Interestingly, enhancing Rb-E2F complex with CDK4/6 inhibition can also significantly redistribute AR-binding sites. These new sites appeared to be enriched for E2F binding sequences, which may further strengthen AR interaction with Rb-E2F complex. Future analyses are required to comprehensively characterize this AR reprogramming induced by CDK4/6 inhibitor treatment.

Another target pathway consistently repressed by high-T is Myc signaling, which also regulates DNA synthesis and cell cycle progression.[63,64] However, the androgen-induced repression effect on Myc signaling appeared to be indirect and much weaker than the effect on E2F signaling. Unlike AR-induced Rb binding, c-Myc chromatin binding was not strongly altered by high-T and was not associated with AR-repressed genes (see Figure 1). Therefore, the indirect suppression effect of high-T on Myc targets is possibly mediated by the transcriptional repression on *MYC* gene[18] and activation on *MXD1* gene (encodes Mad protein, a negative regulator of Myc; see Figure 2F), which promotes Myc/Mad repressor complex.[65] Importantly, our data revealed persistent repression of Myc signaling by the high-T treatment (super high dose) in Rb-depleted CRPC tumors, suggesting that the repression on Myc signaling may play a role in mediating the tumor-suppressive function of high-T in *RB1*-loss CRPC. Therefore, combining high-T with therapies targeting Myc signaling may be a potential combination strategy for treating *RB1*-loss CRPC.

While the high-T treatment in the setting of BAT appeared to be effective in the recent two phase II clinical trials,[10,11] CDK4/6 inhibitor treatment was not promising in treating hormone-sensitive metastatic PCa when it was combined with AR-signaling-inhibition treatment.[53] Therefore, our study provides an important therapeutic strategy to combine CDK4/6 inhibition with high-T treatment in treating Rb-proficient CRPC, and our data from the preclinical studies using PDX models support this strategy (see Figure 7). However, most of the PDX models that we tested appeared to be sensitive to the high-T treatment, and therefore, only a modest enhancing effect was observed with the combination treatment. Future experiments should be done using lower doses of high-T in order to observe a stronger synergetic effect. Interestingly, CDK4/6 inhibitor

and high-T cotarget many pathways in addition to E2F signaling and cell cycle regulations (see Figure 8). These pathways include Myc signaling, DNA repair, and oxidative phosphorylation. The suppression effects on Myc signaling and Myc-regulated homologous recombination pathways by CDK4/6 inhibition have been previously reported in breast and ovarian cancers.[66,67] Therefore, the overall synergetic effect of the combination therapy is likely contributed by the suppression of multiple cancer-promoting pathways. However, biomarkers that can predict the tumor response to high-T or the combination treatment have not been identified. In this study, we suggest that Rb repressor activity, determined by a recently developed Rb-target gene signature,[57] could be used as a prognosis marker to predict the treatment response (see Figures 7E and 7J). Future clinical studies are needed to further validate the use of such biomarkers in the clinical trials of high-T treatment.

In summary, we have determined a central role of Rb/p130-E2F complex in mediating the tumor-suppressive effect of high-T in treating CRPC and demonstrated that the efficacy of high-T treatment depends on Rb activity and that the effect of high-T can be enhanced by CDK4/6 inhibitor treatment in preclinical CRPC models. This study provides a strong rationale for the further development of such combination treatments that can exploit the tumor-suppressor activity of AR in CRPC in clinical trials.

MATERIALS AND METHODS

Cell culture and establishment of stable cell lines are as follows: C4-2 cell lines were obtained from ATCC and were examined for mycoplasma contamination using MycoAlert Mycoplasma Detection Kit (Lonza). Tetracycline-inducible shRNA constructs (pTRIPZ) against non-target control or *RB1* (tet-shRB) were obtained from Dharmacon. Lentifect Purified lentiviral particles of shRNA against *RBL2* were obtained from GeneCopoeia. To establish the stable cell line, C4-2 cells were stably infected with lentivirus-expressing tet-shRB and further selected by puromycin. For establishing RB-KO cell lines, parental C4-2 cells were infected with lentiviral TLCV2-RB1, which expresses doxycycline-inducible Cas9 and single-guide RNA (sgRNA) against RB, followed by further screening and selection for control and knockout clones (sg-RB1: GCTCTGGGTCCTCCT CAGGA). TLCV2-RB1 plasmid was acquired from Addgene (no. 87836) as a gift from Dr. Adam Karpf. All C4-2 and its derived cell lines were maintained in RPMI 1640 medium with reduced steroid hormone (8% charcoal-stripped fetal bovine serum [FBS] [CSS] plus 2% regular FBS). All stable cell lines were maintained using tetracycline-free FBS.

Cell cycle and proliferation assays are as follows: for cell cycle analysis, cells were collected by trypsinization, fixed by 70% ice-cold ethanol for over 3 h, and then stained with Muse Cell Cycle Kit. The stained cells were counted by Guava Muse Cell Analyzer. For proliferation analysis, cells were collected by trypsinization and then examined for cell number and viability by using Muse Count & Viability Kit. The fluorescence signal of the stained cells was measured using Guava Muse Cell Analyzer.

Immunoprecipitation and immunoblotting are as follows: for immunoprecipitation (IP), cells were lysed in Triton lysis buffer supplemented with protein inhibitor cocktails (Thermo Fisher Scientific), followed by brief sonication. Cell lysates were then immunoprecipitated with anti-E2F1 (Abcam) or anti-p130 (Cell Signaling Technology). Proteins were eluted by boiling in Laemmli buffer with 5% beta-mercaptoethanol. For immunoblotting, cells were washed with PBS and then lysed in 2% SDS with boiling. The primary antibodies that were used are anti-Rb (Cell Signaling Technology), anti-p-Rb (Ser780) (Cell Signaling Technology), anti-p130 (Cell Signaling Technology), anti-p-p130 (Ser672) (Abcam), anti-E2F1 (Cell Signaling Technology), and anti-GAPDH (Abcam).

ChIP and ChIP-seq analysis

For conducting ChIP experiments with DHT treatments, cells were grown in hormone-depleted medium (5% CSS) for 3 days and then treated with DHT for 4 h. For the preparation of ChIP, cells were fixed with 1% formaldehyde and lysed by the ChIP lysis buffer (1% SDS, 5 mM EDTA, and 50 mM Tris-HCl pH 8.1). Chromatin was then sheared to ~300-bp fragments using Bioruptor Sonicator (Diagenode). Immunoprecipitation was carried out using anti-Rb antibody (Cell Signaling Technology and BD Pharmingen), anti-Myc (Cell Signaling Technology), anti-AR antibody (Abcam), anti-FOXA1 (EMD Millipore), and anti-p130 antibody (Cell Signaling Technology). Precipitated protein-DNA complexes were then reverse-cross-linked at 65°C, followed by DNA purification. ChIP-seq libraries were constructed using the SMARTer ThruPLEX DNA-Seq Prep Kit (Takara Bio USA). Next-generation sequencing (51 nt, single-end) was performed using Illumina HiSeq2500. ChIP-seq reads were mapped to the hg19 human genome using bwa (v.0.7.9a) with aln and samse sub-commands. Samtools (v.1.2) was used to convert sam files to bam format. The significance of enriched ChIP regions was evaluated by using MACS2 (v.2.1.0).[68] The R package IRanges (v.2.18.3) was used to analyze peak intervals and determine the overlapped regions. Venn diagrams were generated using VennDiagram (v.1.6.20) R package.[69] The signals associated with genomic regions were visualized by using compueMatrix and plotHeatmap tools from deepTools (v.3.3.0).[70] computeMatrix with reference-point mode was used to calculate scores for each genomic region, and plotHeatmap was used to create a heatmap for scores associated with genomic regions. Motif enrichment analysis was performed by using SeqPos with the default setting in Galaxy/Cistrome.[38] Binding and expression target analysis (BETA) was performed by BETA software package (v.1.0.7)[39] with default parameters to integrate ChIP-seq and with differential gene expression to predict direct targets. Peak interval files from MACS2 and differential expression results from limma were used as inputs.

Quantitative real-time PCR and RNA-seq

RNA from the cell lines was extracted with TRIzol reagent (Invitrogen). RNA from tumor tissue samples was extracted by using TissueLyser LT (QIAGEN) and RNeasy Kit (QIAGEN). Quantitative real-time PCR was performed using Fast 1-step Mix (Thermo Fisher Scientific) at QuantStudio 3 PCR machine. All quantitative real-time

PCR results were normalized with GAPDH. All Taqman primers and probes were predesigned by and obtained from Thermo Fisher Scientific.

For RNA-seq, the library preparation was done using TruSeq Stranded mRNA (Illumina). Next-generation sequencing (51 nt, single-end) was performed using Illumina HiSeq2500. Transcriptome sequencing reads were aligned to the human reference genome (hg19) using STAR (v.2.7.2) followed by counting with featureCounts (v.1.6.4) from GRCh37 Ensembl reference. All gene counts were processed with R package limma (v.3.40.6)[71] to evaluate the differential expression using the Benjamini-Hochberg false discovery rate (FDR)-adjusted p value. The expression values were centered and scaled across samples and then displayed using the ComplexHeatmap (v.2.0.0) R package. GSEA was done by using R package fgsea (v.1.10.1). The assession number for ChIP-seq and RNA-seq data generated in this study is GEO: GSE179688.

Xenograft study

All animal experiments were approved by the University of Massachusetts, Boston Institutional Animal Care and Use Committee and were conducted following institutional and national (USA) guidelines. C4-2-tet-shRB cells were resuspended in serum-free RPMI 1640 medium and mixed in 1:1 ratio with Matrigel (BD Biosciences) prior to subcutaneous implantation (2×10^6 cells per injection) on flanks of castrated SCID mice (~4 to 6 weeks old; Taconic). Xenograft tumors, including PDXs, were further passaged in castrated male SCID mice. To silence Rb, mice bearing tumors derived from C4-2-tet-shRB were fed with doxycycline-supplemented food and drinking water. Tumor length (L) and width (W) were measured by caliper at the indicated time, and tumor volumes were calculated ($L \times W^2/2$).

Statistical analysis

Data in bar graphs represent the mean ± SD of at least three biological repeats. Data in the tumor growth curves represent the mean ± SE of at least 4 independent tumor samples. For most studies, statistical analyses were performed using Student's t test by comparing treatment versus vehicle or otherwise as indicated. $p < 0.05$ (*) was considered to be statistically significant. The results for immunoblotting are representative of at least three experiments. Boxplots of signature scores and gene expression were compared using the Wilcoxon test for comparison between two groups of samples. The difference in tumor growth was determined using two-way ANOVA. All other statistical analyses and visualization were performed with R (v.3.6.0) unless otherwise specified.

SUPPLEMENTAL INFORMATION

Supplemental information can be found online at https://doi.org/10.1016/j.ymthe.2022.01.039.

ACKNOWLEDGMENTS

This work is supported by grants from the NIH (R00 CA166507 and R01 CA211350 to C.C., U54 CA156734 to J.A.M., and P01 CA163227 and P50 CA090381 to S.P.B.), DOD (W81XWH-16-1-0445, W81XWH-19-1-0361, and W81XWH-21-1-0267 to C.C. and W81XWH-19-1-0777 to S.G.), CIHR (142246, 152863, 152864, and 159567 to H.H.H.), and Terry Fox Frontiers Program Project Grants (1090 P3 to H.H.H.). The establishment, characterization, and maintenance of the LuCaP PDXs are funded by the NIH (P50 CA097186 and P01 CA163227). M. Liu was supported by the graduate fellowship from Integrative Biosciences Program at University of Massachusetts Boston. W.H., Z.W., and A.B. were supported by CSM (College of Science and Mathematics) Dean's Doctoral Research Fellowship from University of Massachusetts Boston. C.C. is supported by Proposal Development Grant Program from University of Massachusetts Boston. H.H.H. holds the Joey and Toby Tanenbaum Brazilian Ball Chair in Prostate Cancer. H.-M.L. and E.C. are supported by the Institute of Prostate Cancer Research (IPCR).

AUTHOR CONTRIBUTIONS

C.C., S.G., S.P.B., E.C., and W.H. designed the study. W.H., M. Liu, D.H., M. Li, A.A.T., Z.W., A.B., S.G., and H.-M.L. performed experiments and analyzed the results. W.H., D.H., M. Liu, S.P., and J.A.M. performed deep sequencing analyses. C.C. and W.H. wrote the manuscript. All authors discussed the results and commented on the manuscript.

DECLARATION OF INTERESTS

No potential conflicts of interest were disclosed.

REFERENCES

1. Yuan, X., Cai, C., Chen, S., Chen, S., Yu, Z., and Balk, S.P. (2014). Androgen receptor functions in castration-resistant prostate cancer and mechanisms of resistance to new agents targeting the androgen axis. Oncogene *33*, 2815–2825. https://doi.org/10.1038/onc.2013.235.

2. Cai, C., He, H.H., Chen, S., Coleman, I., Wang, H., Fang, Z., Nelson, P.S., Liu, X.S., Brown, M., and Balk, S.P. (2011). Androgen receptor gene expression in prostate cancer is directly suppressed by the androgen receptor through recruitment of lysine-specific demethylase 1. Cancer Cell *20*, 457–471. https://doi.org/10.1016/j.ccr.2011.09.001.

3. Zhao, J.C., Yu, J., Runkle, C., Wu, L., Hu, M., Wu, D., Liu, J.S., Wang, Q., Qin, Z.S., and Yu, J. (2012). Cooperation between Polycomb and androgen receptor during oncogenic transformation. Genome Res. *22*, 322–331. https://doi.org/10.1101/gr.131508.111.

4. Yu, Z., Chen, S., Sowalsky, A.G., Voznesensky, O.S., Mostaghel, E.A., Nelson, P.S., Cai, C., and Balk, S.P. (2014). Rapid induction of androgen receptor splice variants by androgen deprivation in prostate cancer. Clin. Cancer Res. *20*, 1590–1600. https://doi.org/10.1158/1078-0432.CCR-13-1863.

5. Gao, S., Gao, Y., He, H.H., Han, D., Han, W., Avery, A., Macoska, J.A., Liu, X., Chen, S., Ma, F., et al. (2016). Androgen receptor tumor suppressor function is mediated by recruitment of retinoblastoma protein. Cell Rep *17*, 966–976. https://doi.org/10.1016/j.celrep.2016.09.064.

6. Han, D., Chen, S., Han, W., Gao, S., Owiredu, J.N., Li, M., Balk, S.P., He, H.H., and Cai, C. (2019). ZBTB7A mediates the transcriptional repression activity of the androgen receptor in prostate cancer. Cancer Res. *79*, 5260–5271. https://doi.org/10.1158/0008-5472.CAN-19-0815.

7. Chatterjee, P., Schweizer, M.T., Lucas, J.M., Coleman, I., Nyquist, M.D., Frank, S.B., Tharakan, R., Mostaghel, E., Luo, J., Pritchard, C.C., et al. (2019). Supraphysiological androgens suppress prostate cancer growth through androgen receptor-mediated DNA damage. J. Clin. Invest *129*, 4245–4260. https://doi.org/10.1172/JCI127613.

8. Lam, H.M., Nguyen, H.M., Labrecque, M.P., Brown, L.G., Coleman, I.M., Gulati, R., Lakely, B., Sondheim, D., Chatterjee, P., Marck, B.T., et al. (2019). Durable response of enzalutamide-resistant prostate cancer to supraphysiological testosterone is

associated with a multifaceted growth suppression and impaired DNA damage response transcriptomic program in patient-derived xenografts. Eur. Urol. https://doi.org/10.1016/j.eururo.2019.05.042.

9. Schweizer, M.T., Antonarakis, E.S., Wang, H., Ajiboye, A.S., Spitz, A., Cao, H., Luo, J., Haffner, M.C., Yegnasubramanian, S., Carducci, M.A., et al. (2015). Effect of bipolar androgen therapy for asymptomatic men with castration-resistant prostate cancer: results from a pilot clinical study. Sci. translational Med. *7*, 269ra2. https://doi.org/10.1126/scitranslmed.3010563.

10. Teply, B.A., Wang, H., Luber, B., Sullivan, R., Rifkind, I., Bruns, A., Spitz, A., DeCarli, M., Sinibaldi, V., Pratz, C.F., et al. (2018). Bipolar androgen therapy in men with metastatic castration-resistant prostate cancer after progression on enzalutamide: an open-label, phase 2, multicohort study. Lancet Oncol. *19*, 76–86. https://doi.org/10.1016/S1470-2045(17)30906-3.

11. Denmeade, S.R., Wang, H., Agarwal, N., Smith, D.C., Schweizer, M.T., Stein, M.N., Assikis, V., Twardowski, P.W., Flaig, T.W., Szmulewitz, R.Z., et al. (2021). TRANSFORMER: a randomized phase II study comparing bipolar androgen therapy versus enzalutamide in asymptomatic men with castration-resistant metastatic prostate cancer. J. Clin. Oncol. *39*, 1371–1382. https://doi.org/10.1200/JCO.20.02759.

12. Huang, H., Zegarra-Moro, O.L., Benson, D., and Tindall, D.J. (2004). Androgens repress Bcl-2 expression via activation of the retinoblastoma (RB) protein in prostate cancer cells. Oncogene *23*, 2161–2176. https://doi.org/10.1038/sj.onc.1207326.

13. D'Antonio, J.M., Vander Griend, D.J., and Isaacs, J.T. (2009). DNA licensing as a novel androgen receptor mediated therapeutic target for prostate cancer. Endocr. Relat. Cancer *16*, 325–332. https://doi.org/10.1677/ERC-08-0205.

14. Bohrer, L.R., Chen, S., Hallstrom, T.C., and Huang, H. (2010). Androgens suppress EZH2 expression via retinoblastoma (RB) and p130-dependent pathways: a potential mechanism of androgen-refractory progression of prostate cancer. Endocrinology *151*, 5136–5145. https://doi.org/10.1210/en.2010-0436.

15. Chuu, C.P., Kokontis, J.M., Hiipakka, R.A., Fukuchi, J., Lin, H.P., Lin, C.Y., Huo, C., Su, L.C., and Liao, S. (2011). Androgen suppresses proliferation of castration-resistant LNCaP 104-R2 prostate cancer cells through androgen receptor, Skp2, and c-Myc. Cancer Sci. *102*, 2022–2028. https://doi.org/10.1111/j.1349-7006.2011.02043.x.

16. Kregel, S., Kiriluk, K.J., Rosen, A.M., Cai, Y., Reyes, E.E., Otto, K.B., Tom, W., Paner, G.P., Szmulewitz, R.Z., and Vander Griend, D.J. (2013). Sox2 is an androgen receptor-repressed gene that promotes castration-resistant prostate cancer. PLoS One *8*, e53701. https://doi.org/10.1371/journal.pone.0053701.

17. Hsieh, C.L., Botta, G., Gao, S., Li, T., Van Allen, E.M., Treacy, D.J., Cai, C., He, H.H., Sweeney, C.J., Brown, M., et al. (2015). PLZF, a tumor suppressor genetically lost in metastatic castration-resistant prostate cancer, is a mediator of resistance to androgen deprivation therapy. Cancer Res. *75*, 1944–1948. https://doi.org/10.1158/0008-5472.CAN-14-3602.

18. Guo, H., Wu, Y., Nouri, M., Spisak, S., Russo, J.W., Sowalsky, A.G., Pomerantz, M.M., Wei, Z., Korthauer, K., Seo, J.H., et al. (2021). Androgen receptor and MYC equilibration centralizes on developmental super-enhancer. Nat. Commun. *12*, 7308. https://doi.org/10.1038/s41467-021-27077-y.

19. Xiang, Z., Sun, Y., You, B., Zhang, M., Huang, C., Yu, J., You, X., Wu, D., and Chang, C. (2021). Suppressing BCL-XL increased the high dose androgens therapeutic effect to better induce the Enzalutamide-resistant prostate cancer autophagic cell death. Cell Death Dis *12*, 68. https://doi.org/10.1038/s41419-020-03321-z.

20. Dick, F.A., and Rubin, S.M. (2013). Molecular mechanisms underlying RB protein function. Nat. Rev. Mol. Cel. Biol. *14*, 297–306. https://doi.org/10.1038/nrm3567.

21. Giacinti, C., and Giordano, A. (2006). RB and cell cycle progression. Oncogene *25*, 5220–5227. https://doi.org/10.1038/sj.onc.1209615.

22. Robinson, D., Van Allen, E.M., Wu, Y.M., Schultz, N., Lonigro, R.J., Mosquera, J.M., Montgomery, B., Taplin, M.E., Pritchard, C.C., Attard, G., et al. (2015). Integrative clinical genomics of advanced prostate cancer. Cell *161*, 1215–1228. https://doi.org/10.1016/j.cell.2015.05.001.

23. Abida, W., Cyrta, J., Heller, G., Prandi, D., Armenia, J., Coleman, I., Cieslik, M., Benelli, M., Robinson, D., Van Allen, E.M., et al. (2019). Genomic correlates of clinical outcome in advanced prostate cancer. Proc. Natl. Acad. Sci. U S A *116*, 11428–11436. https://doi.org/10.1073/pnas.1902651116.

24. Ku, S.Y., Rosario, S., Wang, Y., Mu, P., Seshadri, M., Goodrich, Z.W., Goodrich, M.M., Labbe, D.P., Gomez, E.C., Wang, J., et al. (2017). Rb1 and Trp53 cooperate to suppress prostate cancer lineage plasticity, metastasis, and antiandrogen resistance. Science *355*, 78–83. https://doi.org/10.1126/science.aah4199.

25. Mu, P., Zhang, Z., Benelli, M., Karthaus, W.R., Hoover, E., Chen, C.C., Wongvipat, J., Ku, S.Y., Gao, D., Cao, Z., et al. (2017). SOX2 promotes lineage plasticity and antiandrogen resistance in TP53- and RB1-deficient prostate cancer. Science *355*, 84–88. https://doi.org/10.1126/science.aah4307.

26. McNair, C., Xu, K., Mandigo, A.C., Benelli, M., Leiby, B., Rodrigues, D., Lindberg, J., Gronberg, H., Crespo, M., De Laere, B., et al. (2018). Differential impact of RB status on E2F1 reprogramming in human cancer. J. Clin. Invest *128*, 341–358. https://doi.org/10.1172/JCI93566.

27. Nyquist, M.D., Corella, A., Coleman, I., De Sarkar, N., Kaipainen, A., Ha, G., Gulati, R., Ang, L., Chatterjee, P., Lucas, J., et al. (2020). Combined TP53 and RB1 loss promotes prostate cancer resistance to a spectrum of therapeutics and confers vulnerability to replication stress. Cell Rep *31*, 107669. https://doi.org/10.1016/j.celrep.2020.107669.

28. Mandigo, A.C., Yuan, W., Xu, K., Gallagher, P., Pang, A., Guan, Y.F., Shafi, A.A., Thangavel, C., Sheehan, B., Bogdan, D., et al. (2021). RB/E2F1 as a master regulator of cancer cell metabolism in advanced disease. Cancer Discov. https://doi.org/10.1158/2159-8290.CD-20-1114.

29. Pfitzenmaier, J., Quinn, J.E., Odman, A.M., Zhang, J., Keller, E.T., Vessella, R.L., and Corey, E. (2003). Characterization of C4-2 prostate cancer bone metastases and their response to castration. J. Bone Miner Res. *18*, 1882–1888. https://doi.org/10.1359/jbmr.2003.18.10.1882.

30. Korenchuk, S., Lehr, J.E., Clean, L.M., Lee, Y.G., Whitney, S., Vessella, R., Lin, D.L., and Pienta, K.J. (2001). VCaP, a cell-based model system of human prostate cancer. In Vivo *15*, 163–168.

31. Cai, C., Wang, H., Xu, Y., Chen, S., and Balk, S.P. (2009). Reactivation of androgen receptor-regulated TMPRSS2:ERG gene expression in castration-resistant prostate cancer. Cancer Res. *69*, 6027–6032. https://doi.org/10.1158/0008-5472.CAN-09-0395.

32. Cai, C., Chen, S., Ng, P., Bubley, G.J., Nelson, P.S., Mostaghel, E.A., Marck, B., Matsumoto, A.M., Simon, N.I., Wang, H., et al. (2011). Intratumoral de novo steroid synthesis activates androgen receptor in castration-resistant prostate cancer and is upregulated by treatment with CYP17A1 inhibitors. Cancer Res. *71*, 6503–6513. https://doi.org/10.1158/0008-5472.CAN-11-0532.

33. Han, W., Gao, S., Barrett, D., Ahmed, M., Han, D., Macoska, J.A., He, H.H., and Cai, C. (2018). Reactivation of androgen receptor-regulated lipid biosynthesis drives the progression of castration-resistant prostate cancer. Oncogene *37*, 710–721. https://doi.org/10.1038/onc.2017.385.

34. Beltran, H., Rickman, D.S., Park, K., Chae, S.S., Sboner, A., MacDonald, T.Y., Wang, Y., Sheikh, K.L., Terry, S., Tagawa, S.T., et al. (2011). Molecular characterization of neuroendocrine prostate cancer and identification of new drug targets. Cancer Discov. *1*, 487–495. https://doi.org/10.1158/2159-8290.CD-11-0130.

35. Svensson, C., Ceder, J., Iglesias-Gato, D., Chuan, Y.C., Pang, S.T., Bjartell, A., Martinez, R.M., Bott, L., Helczynski, L., Ulmert, D., et al. (2014). REST mediates androgen receptor actions on gene repression and predicts early recurrence of prostate cancer. Nucleic Acids Res. *42*, 999–1015. https://doi.org/10.1093/nar/gkt921.

36. Srinivasan, D., Senbanjo, L., Majumdar, S., Franklin, R.B., and Chellaiah, M.A. (2018). Androgen receptor expression reduces stemness characteristics of prostate cancer cells (PC3) by repression of CD44 and SOX2. J. Cell Biochem. https://doi.org/10.1002/jcb.27573.

37. Kim, D.H., Sun, D., Storck, W.K., Welker Leng, K., Jenkins, C., Coleman, D.J., Sampson, D., Guan, X., Kumaraswamy, A., Rodansky, E.S., et al. (2021). BET bromodomain inhibition blocks an AR-repressed, E2F1-activated treatment-emergent neuroendocrine prostate cancer lineage plasticity program. Clin. Cancer Res. https://doi.org/10.1158/1078-0432.CCR-20-4968.

38. Liu, T., Ortiz, J.A., Taing, L., Meyer, C.A., Lee, B., Zhang, Y., Shin, H., Wong, S.S., Ma, J., Lei, Y., et al. (2011). Cistrome: an integrative platform for transcriptional regulation studies. Genome Biol. *12*, R83. https://doi.org/10.1186/gb-2011-12-8-r83.

39. Wang, S., Sun, H., Ma, J., Zang, C., Wang, C., Wang, J., Tang, Q., Meyer, C.A., Zhang, Y., and Liu, X.S. (2013). Target analysis by integration of transcriptome and ChIP-seq data with BETA. Nat. Protoc. *8*, 2502–2515. https://doi.org/10.1038/nprot.2013.150.

40. Araki, K., Nakajima, Y., Eto, K., and Ikeda, M.A. (2003). Distinct recruitment of E2F family members to specific E2F-binding sites mediates activation and repression of the E2F1 promoter. Oncogene *22*, 7632–7641. https://doi.org/10.1038/sj.onc.1206840.

41. Yoshida, K., and Inoue, I. (2004). Regulation of Geminin and Cdt1 expression by E2F transcription factors. Oncogene *23*, 3802–3812. https://doi.org/10.1038/sj.onc.1207488.

42. Prensner, J.R., Chen, W., Han, S., Iyer, M.K., Cao, Q., Kothari, V., Evans, J.R., Knudsen, K.E., Paulsen, M.T., Ljungman, M., et al. (2014). The long non-coding RNA PCAT-1 promotes prostate cancer cell proliferation through cMyc. Neoplasia *16*, 900–908. https://doi.org/10.1016/j.neo.2014.09.001.

43. Bracken, A.P., Pasini, D., Capra, M., Prosperini, E., Colli, E., and Helin, K. (2003). EZH2 is downstream of the pRB-E2F pathway, essential for proliferation and amplified in cancer. EMBO J. *22*, 5323–5335. https://doi.org/10.1093/emboj/cdg542.

44. Sadasivam, S., and DeCaprio, J.A. (2013). The DREAM complex: master coordinator of cell cycle-dependent gene expression. Nat. Rev. Cancer *13*, 585–595. https://doi.org/10.1038/nrc3556.

45. Jiang, J., Pan, Y., Regan, K.M., Wu, C., Zhang, X., Tindall, D.J., and Huang, H. (2012). Androgens repress expression of the F-box protein Skp2 via p107 dependent and independent mechanisms in LNCaP prostate cancer cells. Prostate *72*, 225–232. https://doi.org/10.1002/pros.21430.

46. Cerami, E., Gao, J., Dogrusoz, U., Gross, B.E., Sumer, S.O., Aksoy, B.A., Jacobsen, A., Byrne, C.J., Heuer, M.L., Larsson, E., et al. (2012). The cBio cancer genomics portal: an open platform for exploring multidimensional cancer genomics data. Cancer Discov. *2*, 401–404. https://doi.org/10.1158/2159-8290.CD-12-0095.

47. Gao, J., Aksoy, B.A., Dogrusoz, U., Dresdner, G., Gross, B., Sumer, S.O., Sun, Y., Jacobsen, A., Sinha, R., Larsson, E., et al. (2013). Integrative analysis of complex cancer genomics and clinical profiles using the cBioPortal. Sci. Signal *6*, pl1. https://doi.org/10.1126/scisignal.2004088.

48. Gao, N., Zhang, J., Rao, M.A., Case, T.C., Mirosevich, J., Wang, Y., Jin, R., Gupta, A., Rennie, P.S., and Matusik, R.J. (2003). The role of hepatocyte nuclear factor-3 alpha (Forkhead Box A1) and androgen receptor in transcriptional regulation of prostatic genes. Mol. Endocrinol. *17*, 1484–1507. https://doi.org/10.1210/me.2003-0020.

49. Lupien, M., Eeckhoute, J., Meyer, C.A., Wang, Q., Zhang, Y., Li, W., Carroll, J.S., Liu, X.S., and Brown, M. (2008). FoxA1 translates epigenetic signatures into enhancer-driven lineage-specific transcription. Cell *132*, 958–970. https://doi.org/10.1016/j.cell.2008.01.018.

50. Swinstead, E.E., Miranda, T.B., Paakinaho, V., Baek, S., Goldstein, I., Hawkins, M., Karpova, T.S., Ball, D., Mazza, D., Lavis, L.D., et al. (2016). Steroid receptors reprogram FoxA1 occupancy through dynamic chromatin transitions. Cell *165*, 593–605. https://doi.org/10.1016/j.cell.2016.02.067.

51. Yu, L., Toriseva, M., Tuomala, M., Seikkula, H., Elo, T., Tuomela, J., Kallajoki, M., Mirtti, T., Taimen, P., Bostrom, P.J., et al. (2016). Increased expression of fibroblast growth factor 13 in prostate cancer is associated with shortened time to biochemical recurrence after radical prostatectomy. Int. J. Cancer *139*, 140–152. https://doi.org/10.1002/ijc.30048.

52. Finn, R.S., Crown, J.P., Lang, I., Boer, K., Bondarenko, I.M., Kulyk, S.O., Ettl, J., Patel, R., Pinter, T., Schmidt, M., et al. (2015). The cyclin-dependent kinase 4/6 inhibitor palbociclib in combination with letrozole versus letrozole alone as first-line treatment of oestrogen receptor-positive, HER2-negative, advanced breast cancer (PALOMA-1/TRIO-18): a randomised phase 2 study. Lancet Oncol. *16*, 25–35. https://doi.org/10.1016/S1470-2045(14)71159-3.

53. Palmbos, P.L., Daignault-Newton, S., Tomlins, S.A., Agarwal, N., Twardowski, P., Morgans, A.K., Kelly, W.K., Arora, V.K., Antonarakis, E.S., Siddiqui, J., et al. (2021). A randomized phase II study of androgen deprivation therapy with or without palbociclib in RB-positive metastatic hormone-sensitive prostate cancer. Clin. Cancer Res. https://doi.org/10.1158/1078-0432.CCR-21-0024.

54. Finn, R.S., Martin, M., Rugo, H.S., Jones, S., Im, S.A., Gelmon, K., Harbeck, N., Lipatov, O.N., Walshe, J.M., Moulder, S., et al. (2016). Palbociclib and letrozole in advanced breast cancer. N. Engl. J. Med. *375*, 1925–1936. https://doi.org/10.1056/NEJMoa1607303.

55. Turner, N.C., Slamon, D.J., Ro, J., Bondarenko, I., Im, S.A., Masuda, N., Colleoni, M., DeMichele, A., Loi, S., Verma, S., et al. (2018). Overall survival with palbociclib and fulvestrant in advanced breast cancer. N. Engl. J. Med. *379*, 1926–1936. https://doi.org/10.1056/NEJMoa1810527.

56. Nguyen, H.M., Vessella, R.L., Morrissey, C., Brown, L.G., Coleman, I.M., Higano, C.S., Mostaghel, E.A., Zhang, X., True, L.D., Lam, H.M., et al. (2017). LuCaP prostate cancer patient-derived xenografts reflect the molecular heterogeneity of advanced disease an–d serve as models for evaluating cancer therapeutics. Prostate *77*, 654–671. https://doi.org/10.1002/pros.23313.

57. Han, W., Liu, M., Han, D., Li, M., Toure, A.A., Wang, Z., Besschetnova, A., Patalano, S., Macoska, J.A., Gao, S., et al. (2022). RB1 loss in castration-resistant prostate cancer confers vulnerability to LSD1 inhibition. Oncogene. https://doi.org/10.1038/s41388-021-02135-3.

58. McCartney, A., Migliaccio, I., Bonechi, M., Biagioni, C., Romagnoli, D., De Luca, F., Galardi, F., Risi, E., De Santo, I., Benelli, M., et al. (2019). Mechanisms of resistance to CDK4/6 inhibitors: potential implications and biomarkers for clinical practice. Front Oncol. *9*, 666. https://doi.org/10.3389/fonc.2019.00666.

59. Martin-Belmonte, F., and Perez-Moreno, M. (2011). Epithelial cell polarity, stem cells and cancer. Nat. Rev. Cancer *12*, 23–38. https://doi.org/10.1038/nrc3169.

60. Ellenbroek, S.I., Iden, S., and Collard, J.G. (2012). Cell polarity proteins and cancer. Semin. Cancer Biol. *22*, 208–215. https://doi.org/10.1016/j.semcancer.2012.02.012.

61. Johnstone, C.N., Pattison, A.D., Harrison, P.F., Powell, D.R., Lock, P., Ernst, M., Anderson, R.L., and Beilharz, T.H. (2020). FGF13 promotes metastasis of triple-negative breast cancer. Int. J. Cancer *147*, 230–243. https://doi.org/10.1002/ijc.32874.

62. Bluemn, E.G., Coleman, I.M., Lucas, J.M., Coleman, R.T., Hernandez-Lopez, S., Tharakan, R., Bianchi-Frias, D., Dumpit, R.F., Kaipainen, A., Corella, A.N., et al. (2017). Androgen receptor pathway-independent prostate cancer is sustained through FGF signaling. Cancer Cell *32*, 474–489 e476. https://doi.org/10.1016/j.ccell.2017.09.003.

63. Dominguez-Sola, D., and Gautier, J. (2014). MYC and the control of DNA replication. Cold Spring Harb Perspect. Med. *4*. https://doi.org/10.1101/cshperspect.a014423.

64. Bretones, G., Delgado, M.D., and Leon, J. (2015). Myc and cell cycle control. Biochim. Biophys. Acta *1849*, 506–516. https://doi.org/10.1016/j.bbagrm.2014.03.013.

65. Grandori, C., Cowley, S.M., James, L.P., and Eisenman, R.N. (2000). The Myc/Max/Mad network and the transcriptional control of cell behavior. Annu. Rev. Cell Dev Biol *16*, 653–699. https://doi.org/10.1146/annurev.cellbio.16.1.653.

66. Yi, J., Liu, C., Tao, Z., Wang, M., Jia, Y., Sang, X., Shen, L., Xue, Y., Jiang, K., Luo, F., et al. (2019). MYC status as a determinant of synergistic response to Olaparib and Palbociclib in ovarian cancer. EBioMedicine *43*, 225–237. https://doi.org/10.1016/j.ebiom.2019.03.027.

67. Zhu, X., Chen, L., Huang, B., Li, X., Yang, L., Hu, X., Jiang, Y., Shao, Z., and Wang, Z. (2021). Efficacy and mechanism of the combination of PARP and CDK4/6 inhibitors in the treatment of triple-negative breast cancer. J. Exp. Clin. Cancer Res. *40*, 122. https://doi.org/10.1186/s13046-021-01930-w.

68. Zhang, Y., Liu, T., Meyer, C.A., Eeckhoute, J., Johnson, D.S., Bernstein, B.E., Nusbaum, C., Myers, R.M., Brown, M., Li, W., and Liu, X.S. (2008). Model-based analysis of ChIP-seq (MACS). Genome Biol. *9*, R137. https://doi.org/10.1186/gb-2008-9-9-r137.

69. Chen, H., and Boutros, P.C. (2011). VennDiagram: a package for the generation of highly-customizable Venn and Euler diagrams in R. BMC Bioinformatics *12*, 35. https://doi.org/10.1186/1471-2105-12-35.

70. Ramirez, F., Dundar, F., Diehl, S., Gruning, B.A., and Manke, T. (2014). deepTools: a flexible platform for exploring deep-sequencing data. Nucleic Acids Res. *42*, W187–W191. https://doi.org/10.1093/nar/gku365.

71. Ritchie, M.E., Phipson, B., Wu, D., Hu, Y., Law, C.W., Shi, W., and Smyth, G.K. (2015). Limma powers differential expression analyses for RNA-sequencing and microarray studies. Nucleic Acids Res. *43*, e47. https://doi.org/10.1093/nar/gkv007.

YMTHE, Volume *30*

Supplemental Information

Exploiting the tumor-suppressive activity of the androgen receptor by CDK4/6 inhibition in castration-resistant prostate cancer

Wanting Han, Mingyu Liu, Dong Han, Anthia A. Toure, Muqing Li, Anna Besschetnova, Zifeng Wang, Susan Patalano, Jill A. Macoska, Hung-Ming Lam, Eva Corey, Housheng Hansen He, Shuai Gao, Steven P. Balk, and Changmeng Cai

Supplementary Information Inventory:

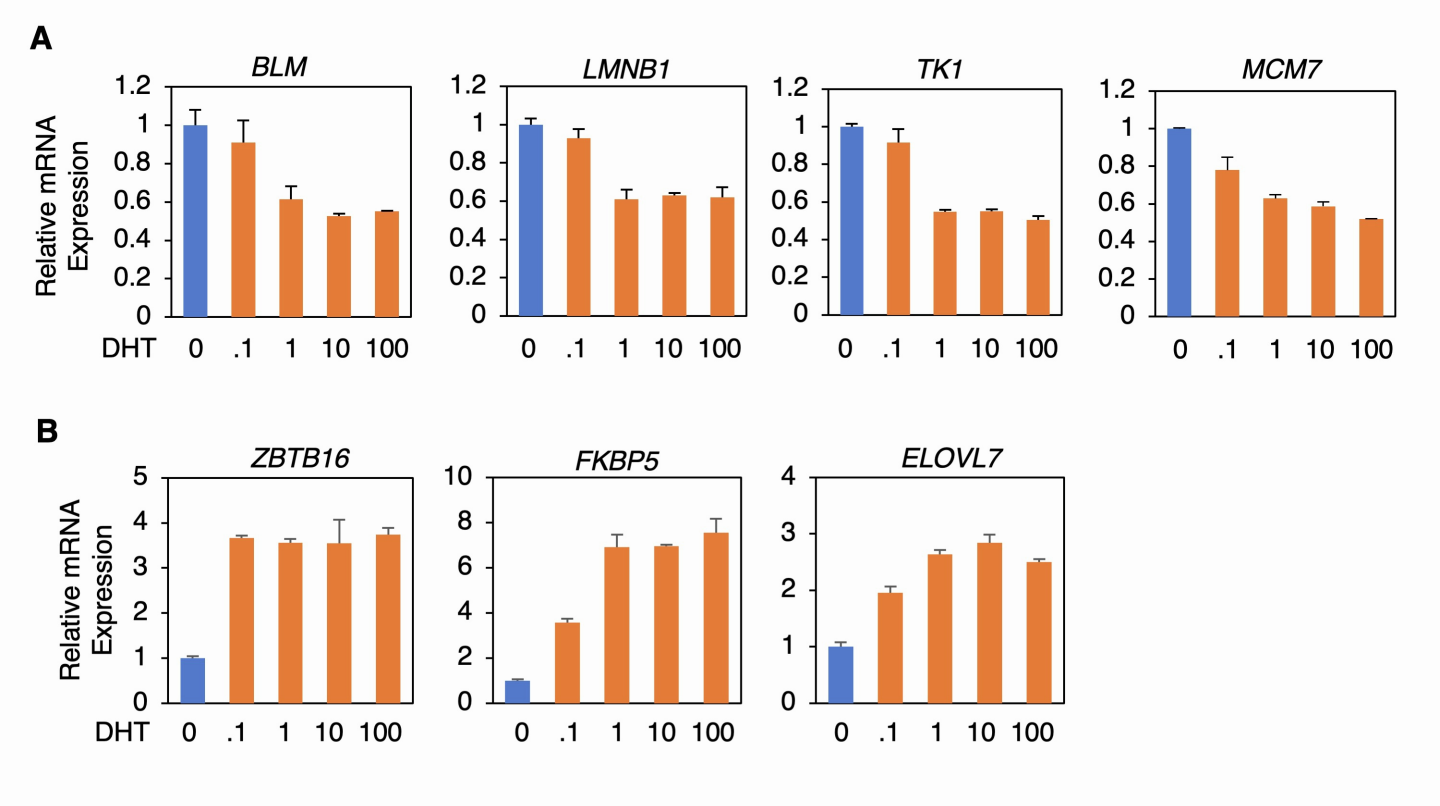

Supplementary Figure S1, related to Figure 1

(**A, B**) C4-2 cells were hormone-depleted for 3d and then treated with DHT (0-100nM) for 24h. qRT-PCR analyses were done to examine the expression of AR-repressed DNA synthesis genes (A) and classic AR-activated genes (B).

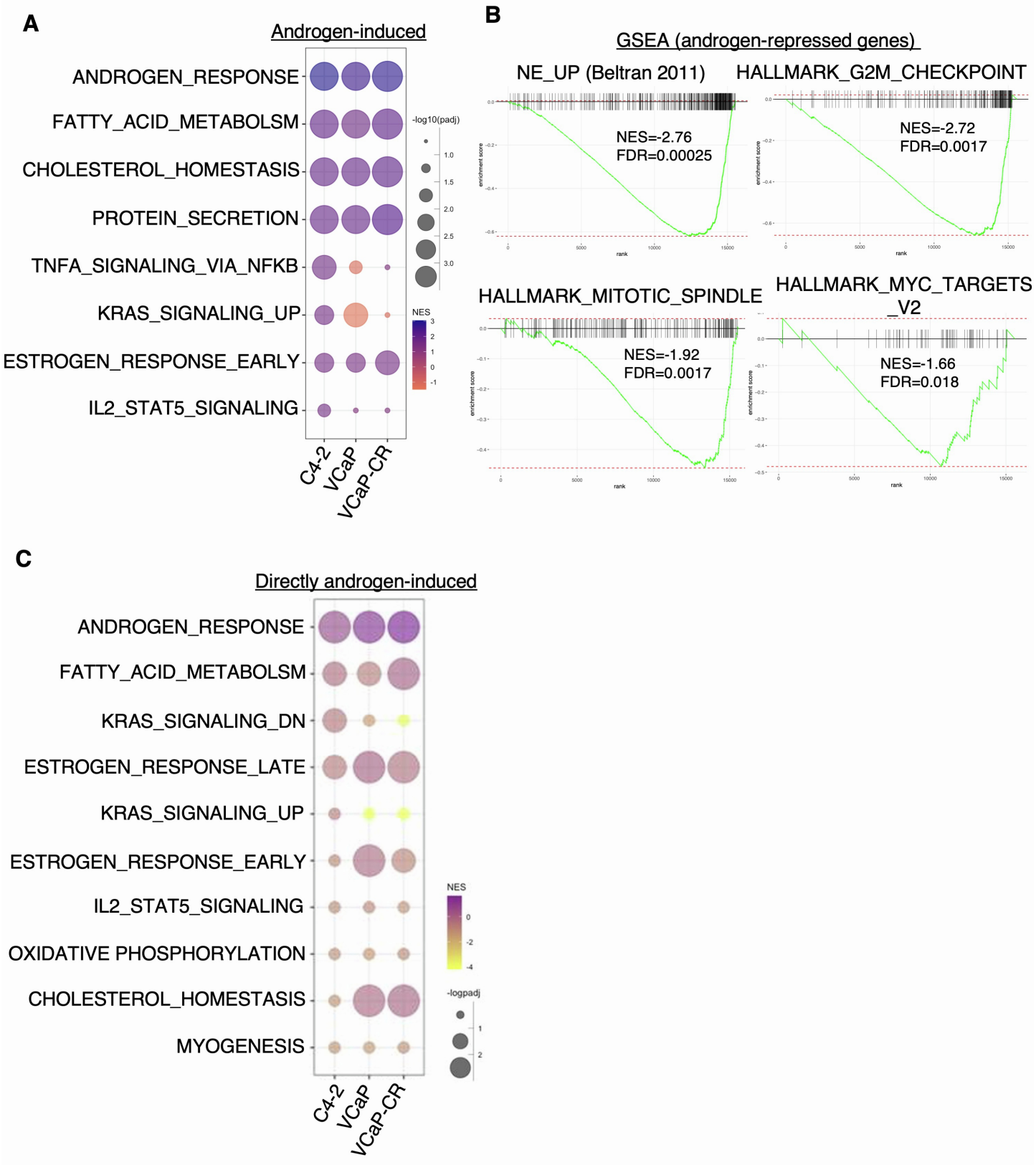
A
Androgen-induced
ANDROGEN_RESPONSE
FATTY_ACID_METABOLSM
CHOLESTEROL_HOMESTASIS
PROTEIN_SECRETION
TNFA_SIGNALING_VIA_NFKB
KRAS_SIGNALING_UP
ESTROGEN_RESPONSE_EARLY
IL2_STAT5_SIGNALING
C4-2
VCaP
VCaP-CR
-log10(padj)
1.0
1.5
2.0
2.5
3.0
NES
3
2
1
0
-1
B
GSEA (androgen-repressed genes)
NE_UP (Beltran 2011)
NES=-2.76
FDR=0.00025
HALLMARK_G2M_CHECKPOINT
NES=-2.72
FDR=0.0017
HALLMARK_MITOTIC_SPINDLE
NES=-1.92
FDR=0.0017
HALLMARK_MYC_TARGETS_V2
NES=-1.66
FDR=0.018
enrichment score
rank
C
Directly androgen-induced
ANDROGEN_RESPONSE
FATTY_ACID_METABOLSM
KRAS_SIGNALING_DN
ESTROGEN_RESPONSE_LATE
KRAS_SIGNALING_UP
ESTROGEN_RESPONSE_EARLY
IL2_STAT5_SIGNALING
OXIDATIVE PHOSPHORYLATION
CHOLESTEROL_HOMESTASIS
MYOGENESIS
C4-2
VCaP
VCaP-CR
NES
0
-2
-4
-logpadj
1
2

Supplementary Figure S2, related to Figure 1

(**A**) Gene Set Enrichment Analysis (GSEA) was done to compare the androgen-induced genes in C4-2-tet-shRB versus VCaP/VCaP-CR cells. (**B**) Enrichments of NE_UP,[1] HALLMARK_G2M_CHECKPOINT, HALLMARK_MITOTIC_SPINDLE, and HALLMARK_MYC_TARGETS_V2 gene sets for AR-repressed genes were plotted. (**C**) GSEA was done to compare directly androgen-induced genes (AR-activated genes with nearby AR binding) in these cells.

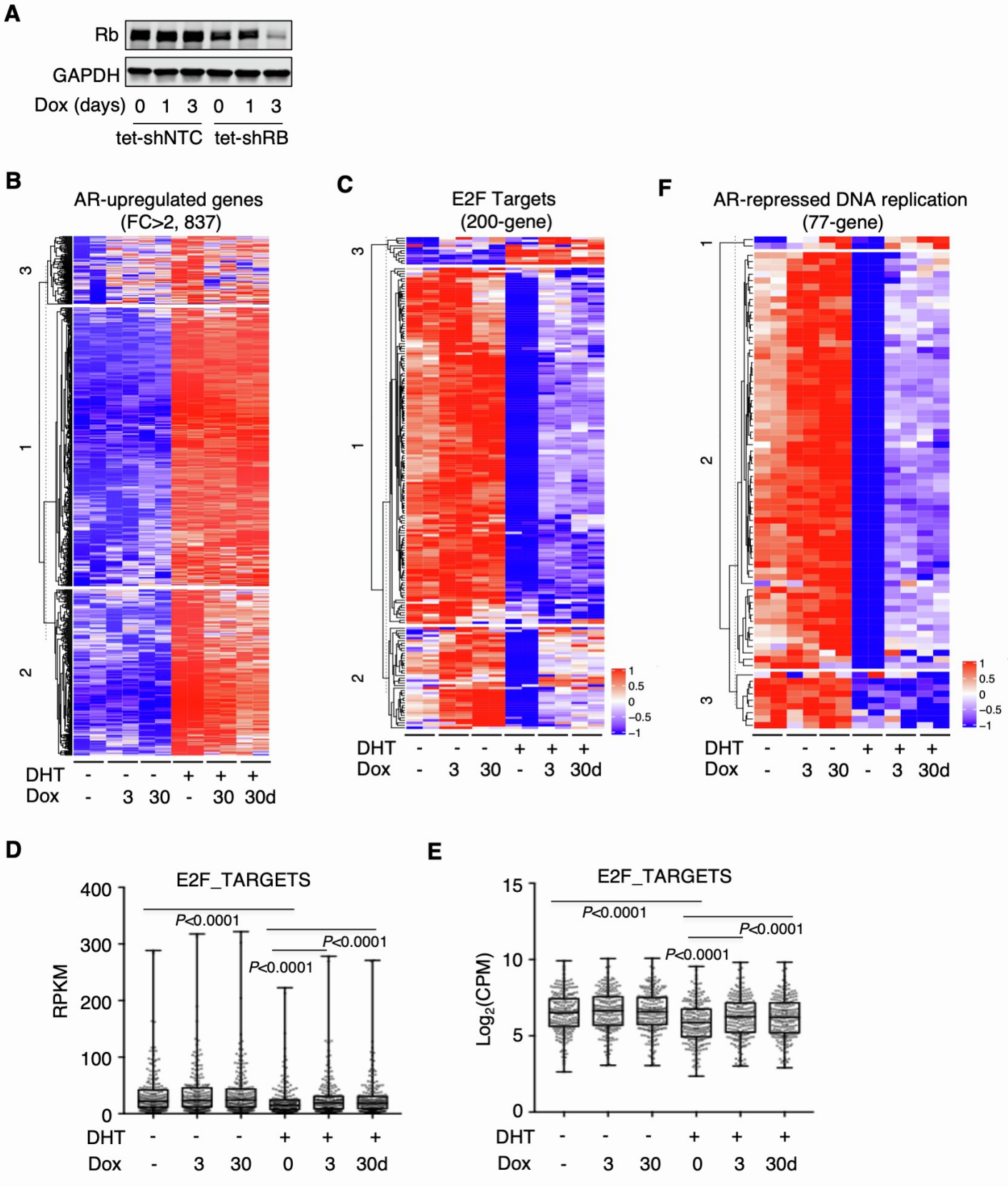
A
Rb
GAPDH
Dox (days) 0 1 3 0 1 3
tet-shNTC tet-shRB
B
AR-upregulated genes
(FC>2, 837)
DHT - - - + + +
Dox - 3 30 - 30 30d
C
E2F Targets
(200-gene)
DHT - - - + + +
Dox - 3 30 - 3 30d
F
AR-repressed DNA replication
(77-gene)
DHT - - - + + +
Dox - 3 30 - 3 30d
D
E2F_TARGETS
RPKM
P<0.0001
P<0.0001
P<0.0001
DHT - - - + + +
Dox - 3 30 0 3 30d
E
E2F_TARGETS
Log2(CPM)
P<0.0001
P<0.0001
P<0.0001
DHT - - - + + +
Dox - 3 30 0 3 30d

Supplementary Figure S3, related to Figure 2

(**A**) Immunoblotting for Rb in the control or C4-2-tet-shRB cells with 0.05μg/ml doxycycline for 0-3d. (**B**, **C**, **F**) Heatmap view for androgen-upregulated genes (B), E2F target genes (C), and previously identified AR repressed DNA replication genes[2] (F). (**D**, **E**) Box plots for the expression of E2F target genes calculated as RPKM (D) or Log_2(CPM) (E) in these samples. Note: RPKM is Reads Per Kilobase of transcript per Million mapped reads and CPM is Counts Per Million mapped reads.

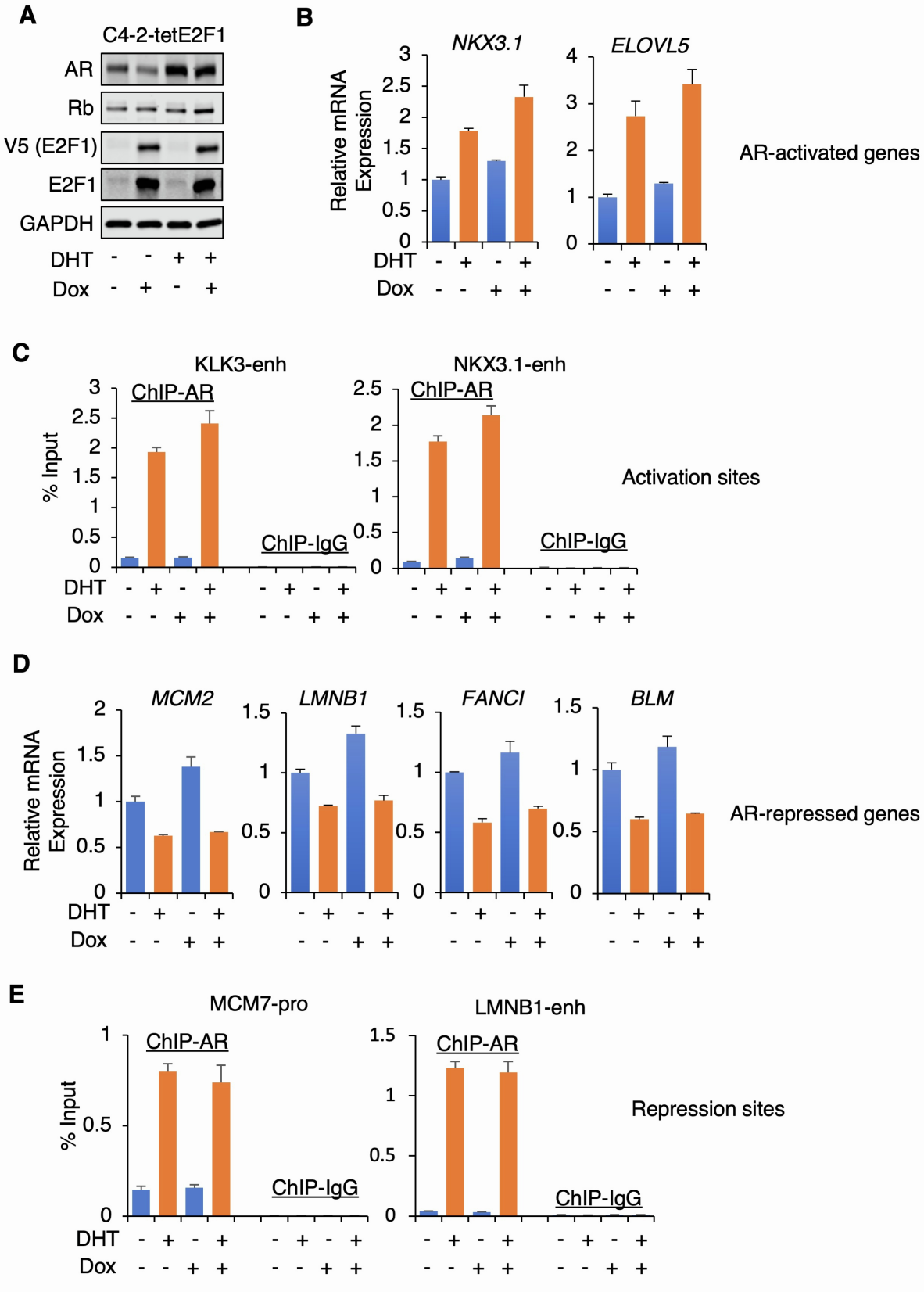
A
C4-2-tetE2F1
AR
Rb
V5 (E2F1)
E2F1
GAPDH
DHT - - + +
Dox - + - +
B
NKX3.1
ELOVL5
Relative mRNA Expression
DHT - + - +
Dox - - + +
AR-activated genes
C
KLK3-enh
NKX3.1-enh
ChIP-AR
ChIP-IgG
% Input
DHT - + - + - + - +
Dox - - + + - - + +
Activation sites
D
MCM2
LMNB1
FANCI
BLM
Relative mRNA Expression
DHT - + - +
Dox - - + +
AR-repressed genes
E
MCM7-pro
LMNB1-enh
ChIP-AR
ChIP-IgG
% Input
DHT - + - + - + - +
Dox - - + + - - + +
Repression sites

Supplementary Figure S4, related to Figure 2

(**A**) Immunoblotting for indicated proteins in C4-2-tetE2F1 cells (expressing doxycycline-regulated V5-tagged E2F1) treated with or without DHT (10nM, 24h) or doxycycline (0.25μg/ul, 3d). (**B**, **D**) qRT-PCR for AR-activated genes (B) and AR-repressed DNA synthesis genes (D). (**C**, **E**) C4-2-tetE2F1 cells were pretreated with doxycycline (3d) and/or treated with DHT (10nM, 4h). ChIP-qPCR for AR binding was examined at AR activation sites (C) or AR repression sites (E).

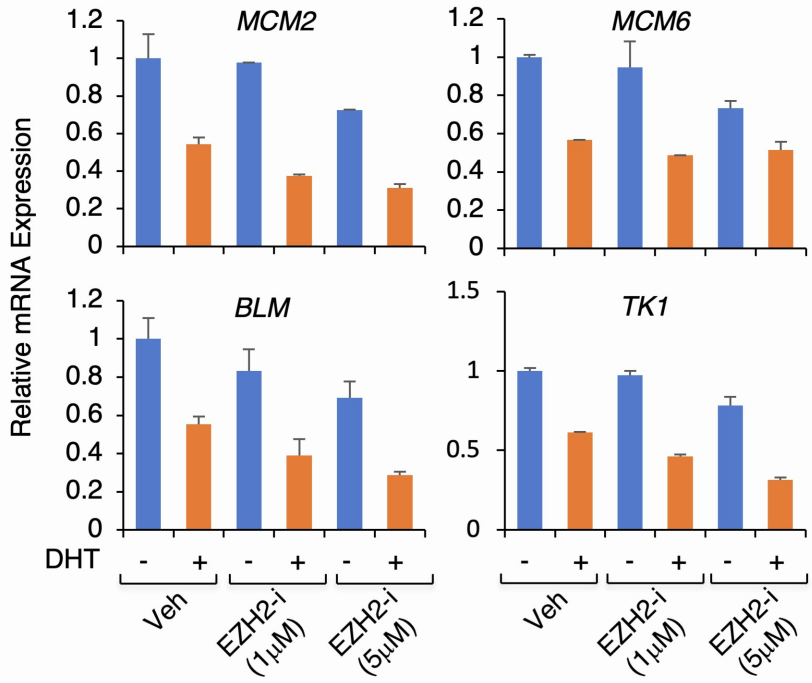

Supplementary Figure S5, related to Figure 2

qRT-PCR for a panel of AR-repressed DNA synthesis genes in C4-2 cells treated with DHT (10nM, 24h) and EZH2 inhibitor GSK126 (0-5μM, 24h).

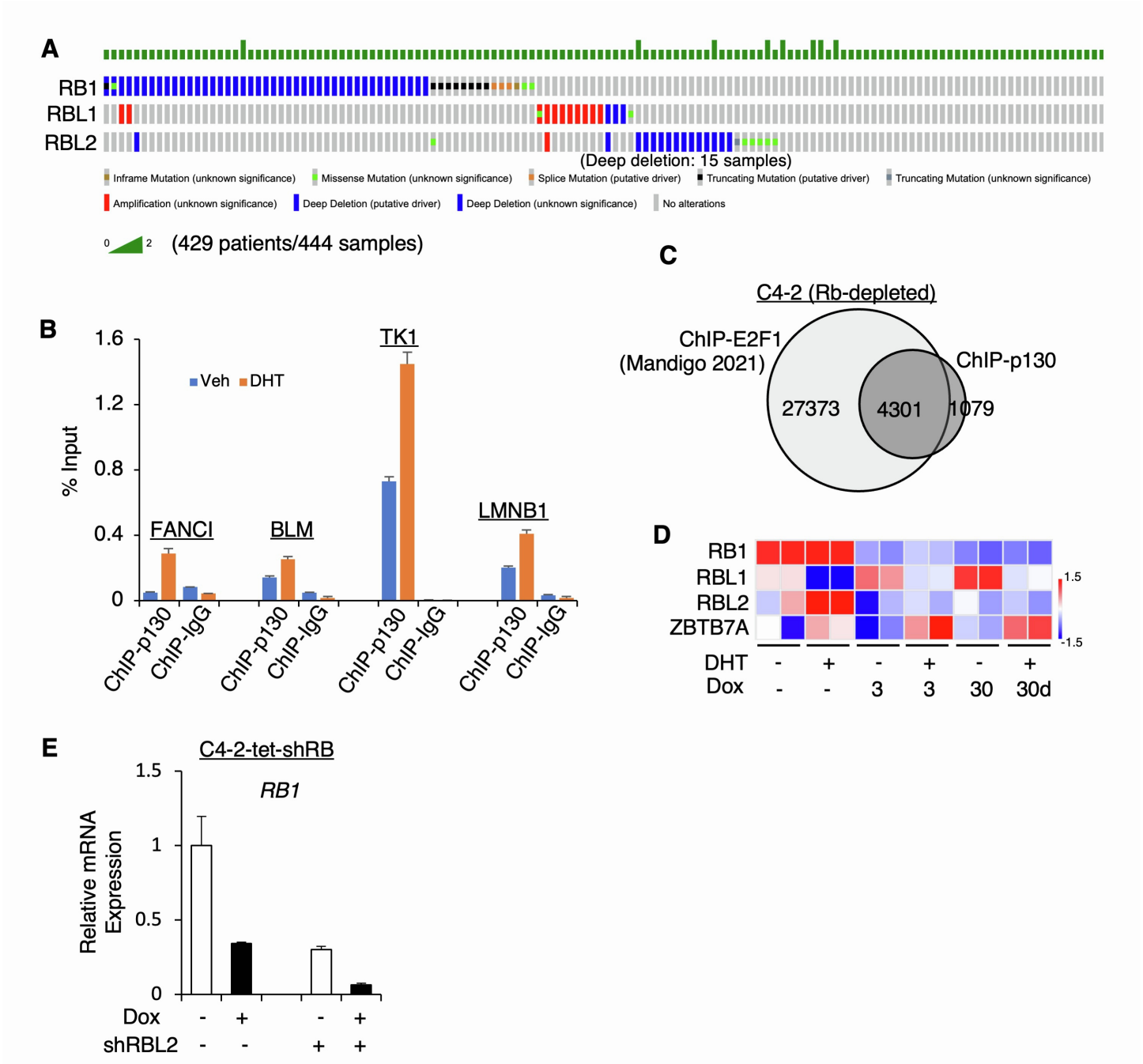

Supplementary Figure S6, related to Figure 3**.**

(**A**) Genomic alterations of *RB1*, *RBL1*, and *RBL2* in SU2C mCRPC dataset (data were analyzed using cBioPortal).[3-5] (**B**) ChIP-qPCR for p130 in C4-2-tet-shRB cells treated with DHT (10nM, 4h). (**C**) The Venn diagram for p130 (C4-2-tet-shRB with doxycycline) and E2F1 (C4-2 with *RB1* silencing)[6] overlapping binding peaks under Rb-depleted condition. (**D**) Heatmap view for the expression levels of *RB1*, *RBL1*, *RBL2*, and

ZBTB7A in C4-2-tet-shRB cells. (**E**) qRT-PCR for *RB1* expression in C4-2-tet-shRB cells treated with doxycycline or stably infected with shRBL2.

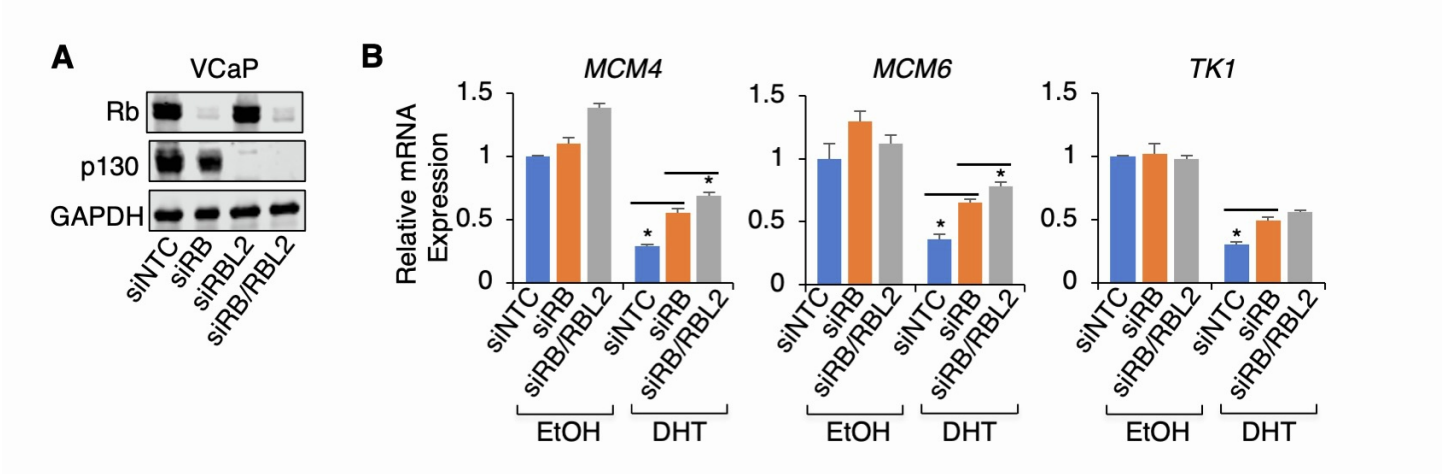

Supplementary Figure S7, related to Figure 3**.**

(**A**) Immunoblotting for Rb and p130 in VCaP cells transfected with siNTC, siRB, siRBL2 (encodes p130), or the combination (3d). (**B**) qRT-PCR for AR-repressed genes in VCaP cells transfected with siNTC, siRB, or siRB+siRBL2 and treated with/out DHT (10nM, 24h).

S**upplementary Figure S8**, related to Figure 4.

(**A**) A Venn diagram for AR-activated genes and the gene annotation of the “lost” AR sites. (**B**) Box plots for the expression levels of AR-activated genes containing at least one “lost” AR site in C4-2-tet-shRB cells.

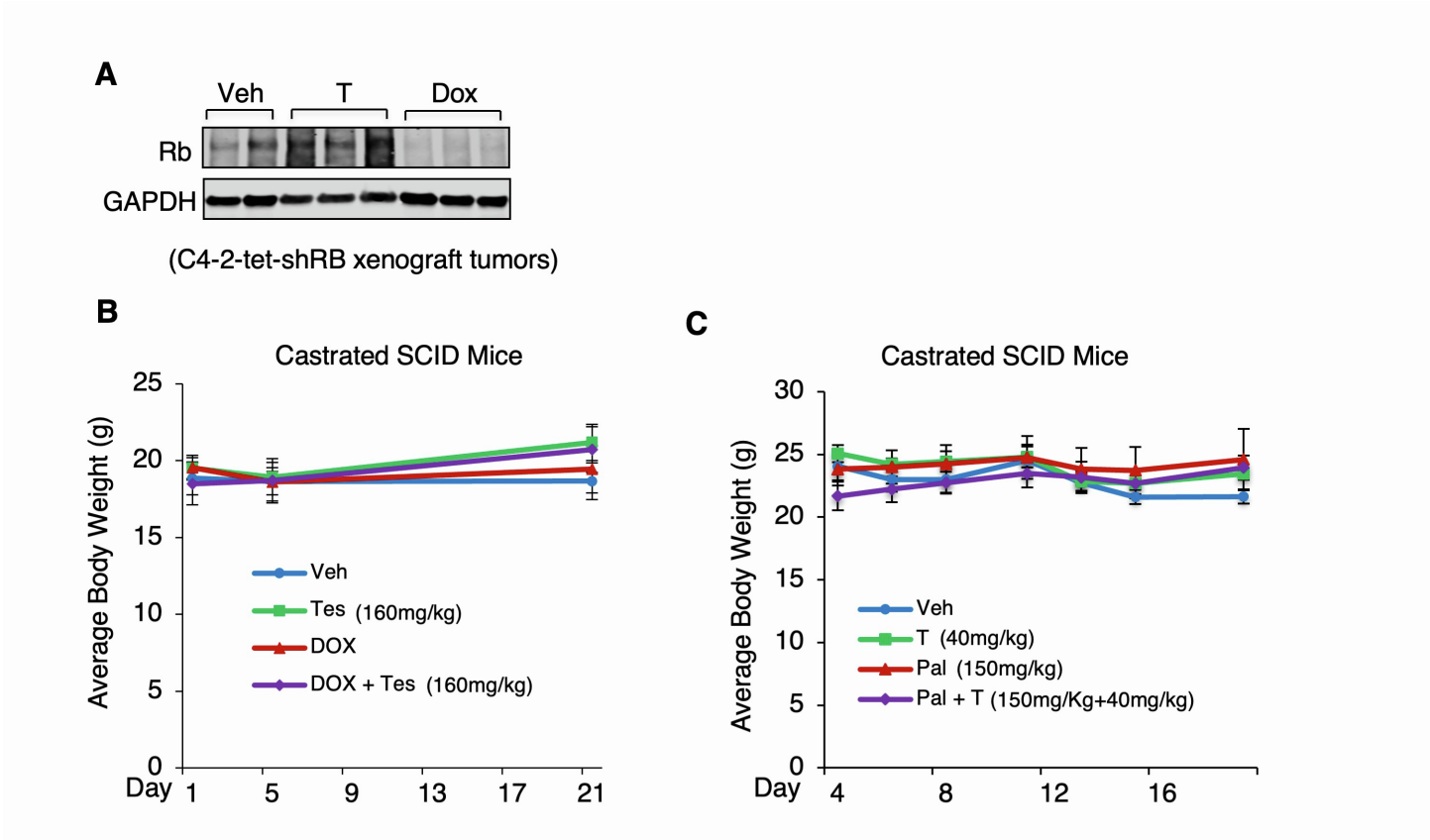

Supplementary Figure S9, related to Figure 5.

(**A**) Immunoblotting for Rb expression in C4-2-tet-shRB xenograft tumor samples from tumor-bearing mice treated with vehicle, 160mg/kg testosterone, and doxycycline supplemented diet. (**B, C**) Bodyweight for castrated male SCID mice receiving daily testosterone (40mg/kg or 160mg/kg) or palbociclib (150mg/kg).

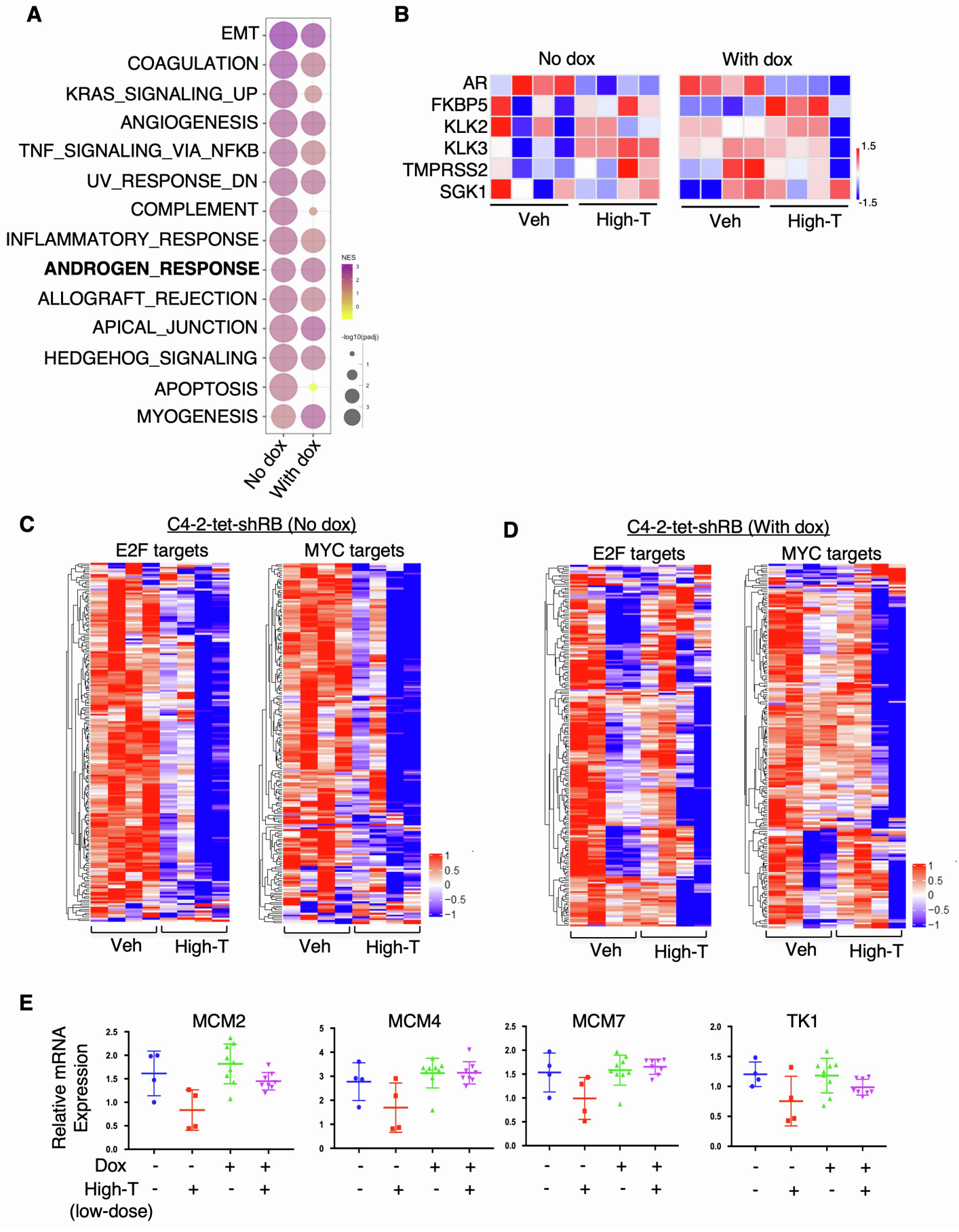
A
EMT
COAGULATION
KRAS_SIGNALING_UP
ANGIOGENESIS
TNF_SIGNALING_VIA_NFKB
UV_RESPONSE_DN
COMPLEMENT
INFLAMMATORY_RESPONSE
ANDROGEN_RESPONSE
ALLOGRAFT_REJECTION
APICAL_JUNCTION
HEDGEHOG_SIGNALING
APOPTOSIS
MYOGENESIS
No dox
With dox
NES
-log10(padj)
B
No dox
With dox
AR
FKBP5
KLK2
KLK3
TMPRSS2
SGK1
Veh
High-T
Veh
High-T
1.5
-1.5
C
C4-2-tet-shRB (No dox)
E2F targets
MYC targets
Veh
High-T
Veh
High-T
D
C4-2-tet-shRB (With dox)
E2F targets
MYC targets
Veh
High-T
Veh
High-T
E
Relative mRNA Expression
MCM2
MCM4
MCM7
TK1
Dox
High-T (low-dose)

Supplementary Figure S10, related to Figure 6.

(**A**) GSEA was done to compare the androgen-induced genes in Rb-proficient tumors versus Rb-deficient tumors. (**B**) Heatmap view for the expression levels of *AR* and a panel of canonical AR-activated genes in the tumor tissues. (**C**, **D**) Heatmap view for E2Fs target genes and Myc target genes in Rb-proficient (C) versus Rb-deficient tumors (D). (**E**) qRT-PCR for a panel of AR-repressed E2F targets in tumor tissues.

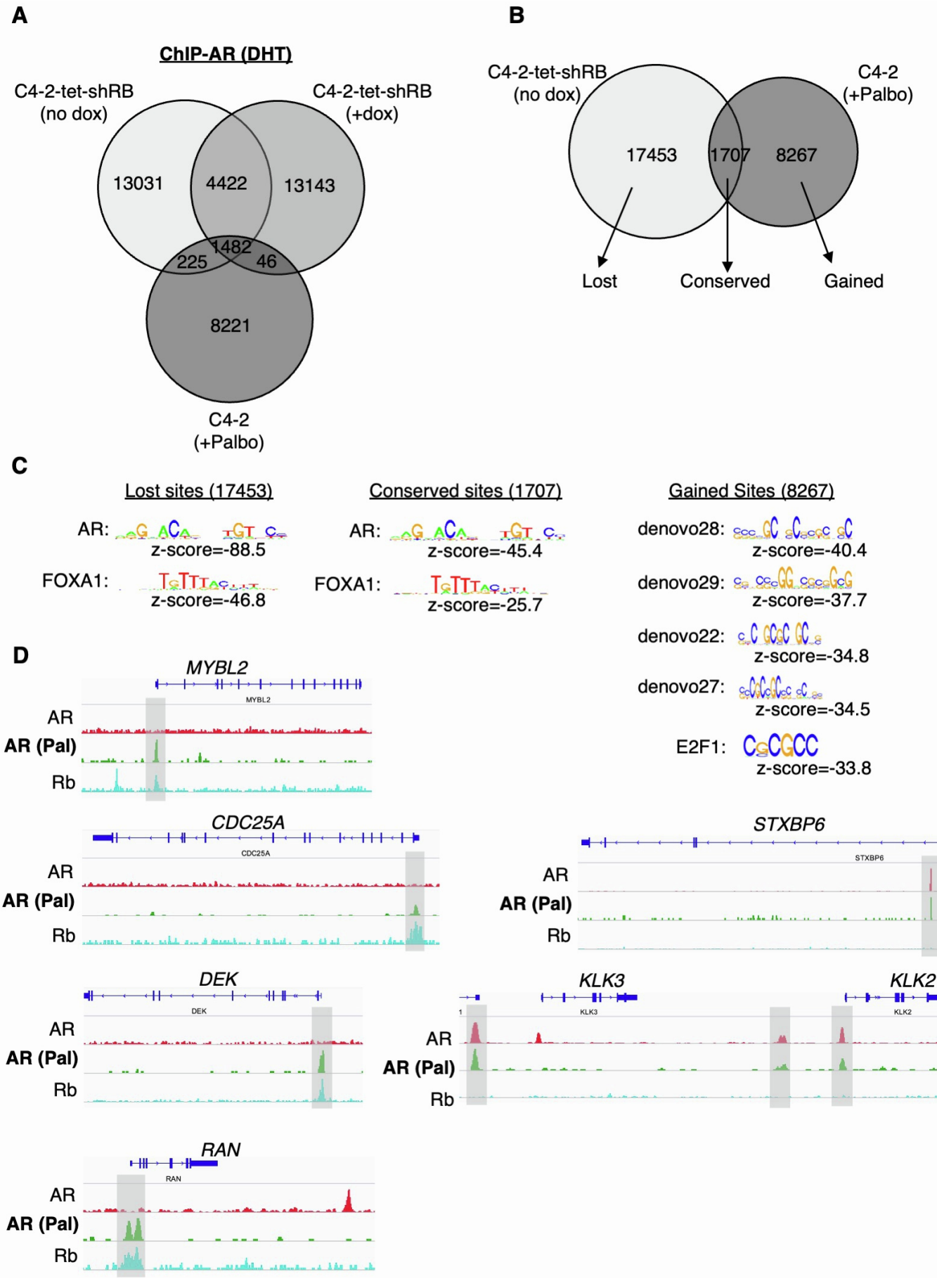
A
ChIP-AR (DHT)
C4-2-tet-shRB (no dox)
C4-2-tet-shRB (+dox)
C4-2 (+Palbo)
13031
4422
13143
1482
225
46
8221
B
C4-2-tet-shRB (no dox)
C4-2 (+Palbo)
17453
1707
8267
Lost
Conserved
Gained
C
Lost sites (17453)
Conserved sites (1707)
Gained Sites (8267)
AR:
z-score=-88.5
FOXA1:
z-score=-46.8
AR:
z-score=-45.4
FOXA1:
z-score=-25.7
denovo28:
z-score=-40.4
denovo29:
z-score=-37.7
denovo22:
z-score=-34.8
denovo27:
z-score=-34.5
E2F1:
z-score=-33.8
D
MYBL2
CDC25A
STXBP6
DEK
KLK3
KLK2
RAN
AR
AR (Pal)
Rb

Supplementary Figure S11, related to Figure 7.

(**A**, **B**) ChIP-seq of AR was done in C4-2 cells treated with palbociclib (1μM, 24h) and DHT (10nM, 4h). 9,974 high-confidence peaks were identified using MACS and a Venn diagram was shown to compare AR binding sites under this treatment with AR bindings in C4-2-tet-shRB cells treated with/out doxycycline (3d) and DHT (10nM, 4h). (**B**) “Lost”, “conserved”, and “gained” sites were identified by comparing ChIP-AR peaks under palbociclib+DHT treatment versus DHT only. (**C**) Motif enrichment analysis for these three groups of AR binding sites. (**D**) Examples for gene loci with "gained” AR binding (left) and “conserved” AR binding. Note: STXBP6 is a previously identified AR repressed gene that is not regulated by Rb, and KLK2/KLK3 are classical AR-activated genes.

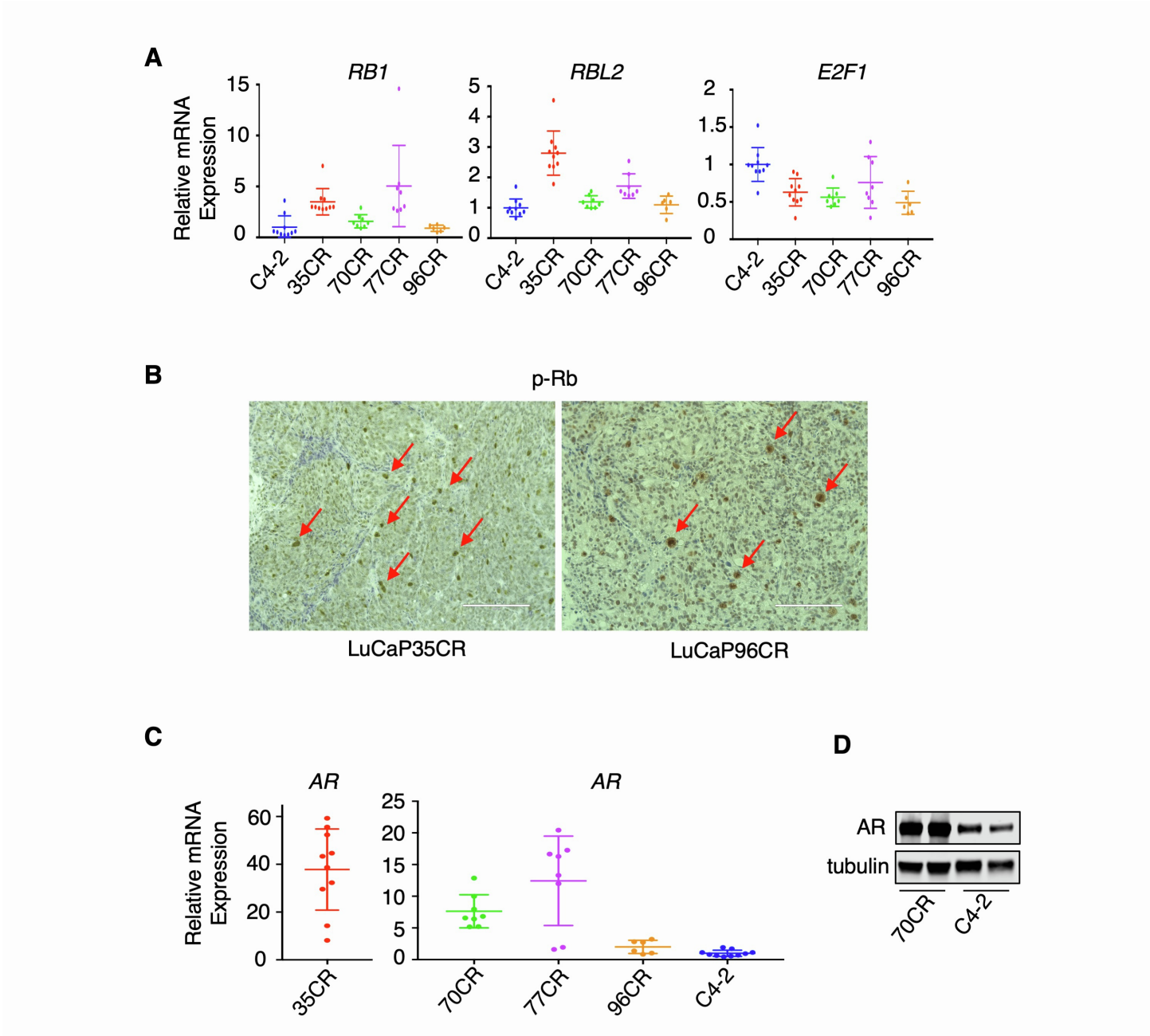

Supplementary Figure S12, related to Figure 7.

(**A**) qRT-PCR for the mRNA expression of indicated genes in tumor samples from C4-2 xenograft and LuCaP PDXs. (**B**) Immunohistochemistry staining of p-Rb (Ser780) in tumor samples from the LuCaP35CR and LuCaP96CR (red arrows indicate cells with high levels of p-Rb). (**C**) qRT-PCR for AR mRNA expression in tumor samples from C4-2 xenograft and LuCaP PDXs. (**D**) Immunoblotting for AR in 70CR and C4-2 xenograft tumor samples.

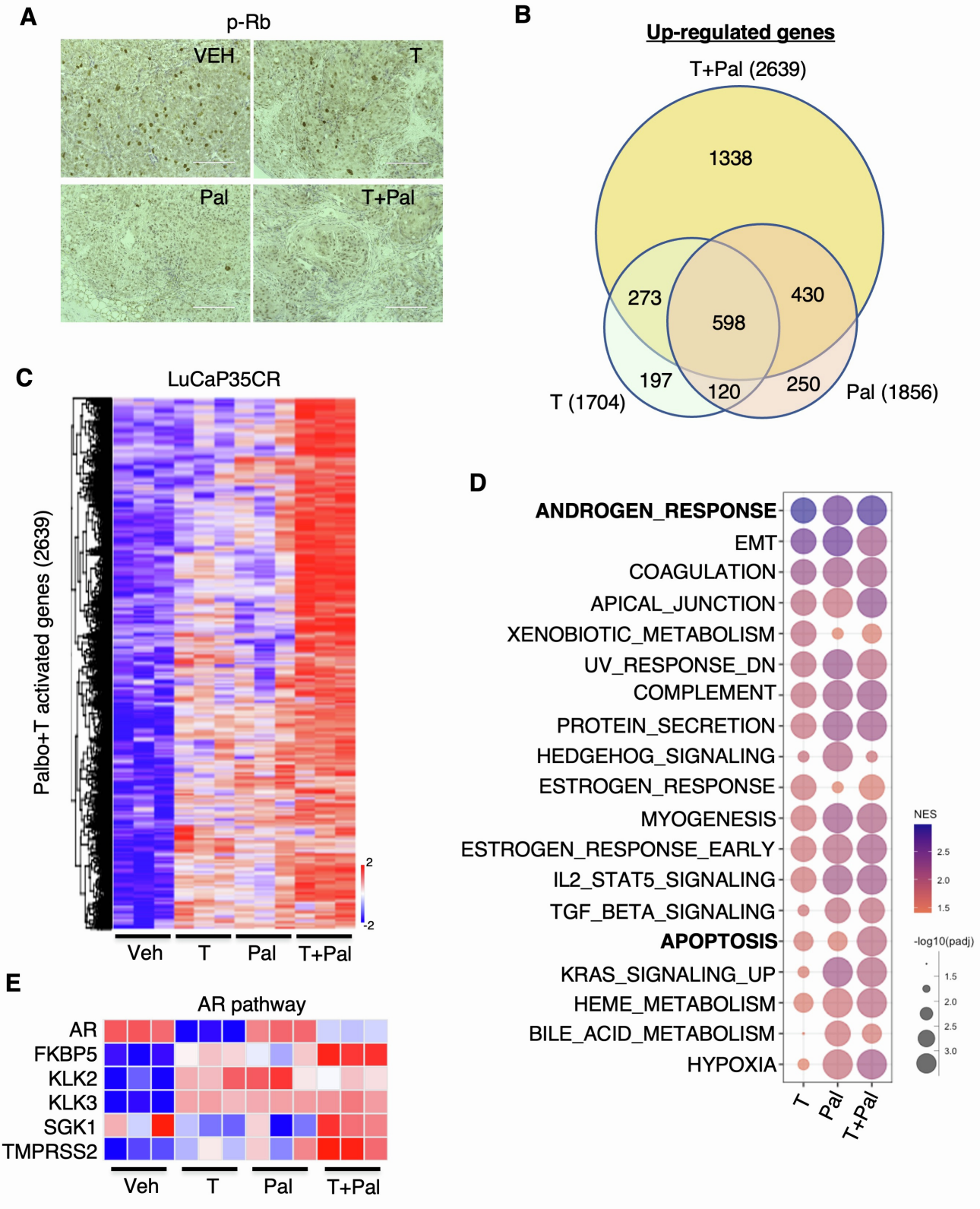
A
p-Rb
VEH
T
Pal
T+Pal
B
Up-regulated genes
T+Pal (2639)
1338
273
430
598
197
120
250
T (1704)
Pal (1856)
C
LuCaP35CR
Palbo+T activated genes (2639)
2
-2
Veh
T
Pal
T+Pal
D
ANDROGEN_RESPONSE
EMT
COAGULATION
APICAL_JUNCTION
XENOBIOTIC_METABOLISM
UV_RESPONSE_DN
COMPLEMENT
PROTEIN_SECRETION
HEDGEHOG_SIGNALING
ESTROGEN_RESPONSE
MYOGENESIS
ESTROGEN_RESPONSE_EARLY
IL2_STAT5_SIGNALING
TGF_BETA_SIGNALING
APOPTOSIS
KRAS_SIGNALING_UP
HEME_METABOLISM
BILE_ACID_METABOLISM
HYPOXIA
T
Pal
T+Pal
NES
2.5
2.0
1.5
-log10(padj)
1.5
2.0
2.5
3.0
E
AR pathway
AR
FKBP5
KLK2
KLK3
SGK1
TMPRSS2
Veh
T
Pal
T+Pal

Supplementary Figure S13, related to Figure 8.

(**A**) Immunohistochemistry staining of p-Rb (Ser780) in tumor samples from the LuCaP35CR study. (**B**) A Venn diagram for high-T-activated genes, palbociclib-activated genes, and the combination treatment-activated genes. (**C**) Heatmap view for the combination treatment-activated genes in all tumor samples. (**D**) GSEA for the upregulated genes by single treatments versus the combination treatment. (**E**) Heatmap view for the expression levels of *AR* and a panel of canonical AR-activated genes in the tumor tissues.

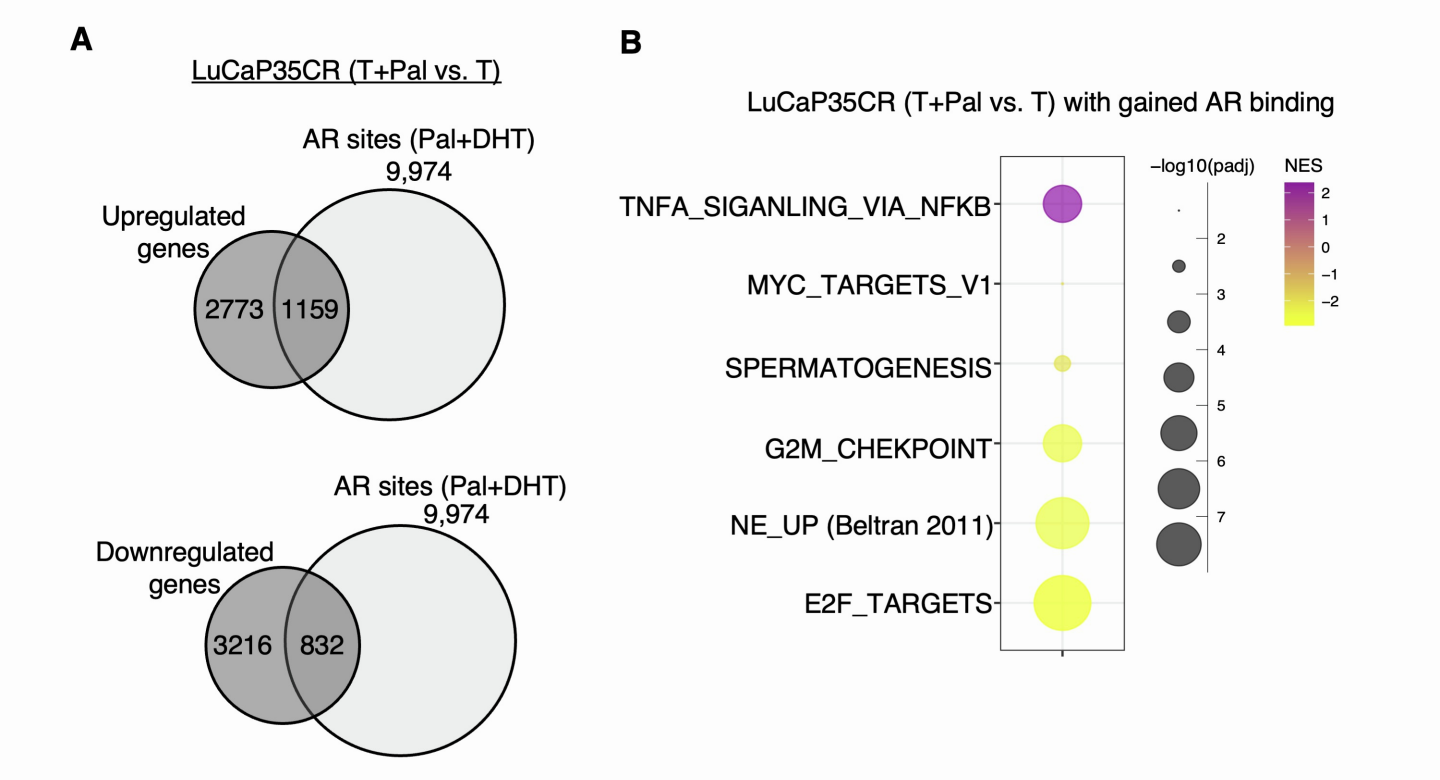

Supplementary Figure S14, related to Figure 8.

(**A**) Identification of up/down-regulated genes (fold-change>1.5) by the combination treatment versus testosterone alone and associated with nearby AR binding sites determined in C4-2 cells treated with DHT+palbociclib. (**B**) GSEA for these up/down-regulated genes.

Supplementary Table S1, related to Figure 2

E2F target gene (200) expression (RPKM) in C4-2-tet-shRB cells. Note: DHT-downregulated genes (fold-change < 1.5) are highlighted in red.

SUPPLEMENTARY METHODS

ChIP-seq analysis

The preliminary sequencing output is supplied in FASTQ format. FastQC (version 0.11.9) was then used to check sequence quality. ChIP-sequencing reads were mapped to the hg19 human genome using bwa (version 0.7.9a) with aln and samse sub-commands. When processing bwa aln, the first 32 subsequences were taken as seed and the parameter for reads trimming is 5 (-l 32 -q 5). Samtools (version 1.2) was used to convert sam files to bam format. The significance of enriched ChIP regions was evaluated by using MACS2 (version 2.1.0)[7] with fix-bimodal turned on and extend size set as 100 (--bw 250 –mfold 10 30 –fix-bimodal –extsize 100). bedGraph files generated from MACS2 were converted into bigwig files with UCSC tools (version 369) as follows: bedGraph files were sorted by bedSort, then clipped with bedClip and converted to bigwig format using bedGraphToBigWig. The import.bed function from R package rtracklayer (version 1.44.4) and the findOverlaps function from R package IRanges (version 2.18.3) were used to analyze peak intervals and determine the overlapped regions. All Venn diagrams were generated using VennDiagram (version 1.6.20) R package.[8] The signals associated with genomic regions were visualized by using compueMatrix and plotHeatmap tools from deepTools (version 3.3.0).[9] computeMatrix with reference-point mode was used to calculate scores for each genomic region, and plotHeatmap was used to create a heatmap for scores associated with genomic regions. Motif enrichment analysis was performed by using SeqPos with the default setting in Galaxy/Cistrome.[10] The top 5000 peaks were determined by ranking $-\log_{10}$(p-value) from MACS results. Binding and Expression Target Analysis (BETA) was performed by BETA software package (version 1.0.7)[11] with default parameters to integrate ChIP-seq with differential gene expression to predict direct targets. Peak interval files from MACS2 and differential expression results from limma were used as inputs.

RNA-seq analysis

Transcriptome-sequencing reads were aligned to the human reference genome (hg19) using STAR (version 2.7.2) followed by counting with featureCounts (version 1.6.4) from GRCh37 Ensembl reference. Genes that were not expressed at a level greater than or equal to 1 count per million reads were excluded from further

analysis. All gene counts were processed with R package limma (3.40.6)[12] to evaluate the differential expression using the Benjamini–Hochberg false discovery rate (FDR)-adjusted *P*-value. The expression values were centered and scaled across samples and then displayed using ComplexHeatmap (version 2.0.0) R package. Gene Set Enrichment Analysis (GSEA) was conducted using pre-ranked gene lists by R package fgsea (version 1.10.1). The top pathways (*P*-value<0.05) ranked by normalized enrichment scores (NES) were plotted for visualization. Gene sets were considered significantly enriched with FDR *q*-value<0.25 and *p*-value<0.05. For identification of AR regulated genes, AR-upregulated and AR-downregulated genes were determined by fold-change>2 and *P*-value<0.05 in the comparison of C4-2-tet-shRB cells (no doxycycline) with DHT treatment versus those with ethanal treatment and with nearby AR peaks found in control C4-2 cells in the presence of DHT. The steps to generate noncanonical AR-regulated genes are: (i) genes were selected by fold-change>1.5 and *P*-value<0.05 in the comparison of short-term *RB1*-silenced cells with DHT versus ethanal; (ii) these genes were further filtered based on the condition that the fold-change of AR-regulated gene expression after *RB1* silencing versus control is great than 2; (iii) the final gene set was generated by examining whether the gene contains “gained” AR binding in C4-2-tet-shRB cells (with doxycycline) in the presence of DHT.

ChIP-qPCR

For preparation of ChIP, cells were fixed with 1% formaldehyde and then lysed by the ChIP lysis buffer (1% SDS, 5 mM EDTA, 50 mM Tris–HCl pH 8.1). Chromatin was then sheared to 500-800 bp fragments using Bioruptor Sonicator (Diagenode). Immunoprecipitation was carried out using anti-p130 antibody (Cell Signaling). DNA fragments were purified and analyzed by qPCR using SYBR Green (Thermo Fisher Scientific) with primer sets of MCM-pro, TK1-pro, LMNB1-pro, FANCI-pro, BLM-enh, KLK3-enh, NKX3.1-enh (listed previously).[2]

Quantitative RT-PCR

RNA from the cell line was extracted with TRIzol reagent (Invitrogen) following the manufacturer's instruction. For RNA from tumor tissue samples, ~30 mg of tumor tissue was homogenized by TissueLyser LT (Qiagen) with one 5 mm bead, and then followed by using RNeasy Kit (Qiagen) to isolate total RNAs. 20 ng of total RNA was

used for quantitative real-time PCR (qRT-PCR) with Fast 1-step Mix (Thermo Fisher Scientific) using QuantStudio 3. All qRT-PCR data were normalized with an internal control GAPDH and quantitated using ΔΔCt method. Taqman primers and probes used in this study were all predesigned by and obtained from Thermo Fisher Scientific.

Immunohistochemistry staining

Immunohistochemistry (IHC) staining was performed on formalin-fixed paraffin-embedded tumor tissue sections using anti-p-Rb (Ser780) antibody (Cell Signaling). IHC was performed by iHisto.

SUPPLEMENTARY REFERENCES

1. Beltran, H., Rickman, D.S., Park, K., Chae, S.S., Sboner, A., MacDonald, T.Y., Wang, Y., Sheikh, K.L., Terry, S., Tagawa, S.T., Dhir, R., et al. (2011). Molecular characterization of neuroendocrine prostate cancer and identification of new drug targets. Cancer Discov *1*, 487-495. 10.1158/2159-8290.CD-11-0130.
2. Gao, S., Gao, Y., He, H.H., Han, D., Han, W., Avery, A., Macoska, J.A., Liu, X., Chen, S., Ma, F., Chen, S., et al. (2016). Androgen Receptor Tumor Suppressor Function Is Mediated by Recruitment of Retinoblastoma Protein. Cell Rep *17*, 966-976. 10.1016/j.celrep.2016.09.064.
3. Cerami, E., Gao, J., Dogrusoz, U., Gross, B.E., Sumer, S.O., Aksoy, B.A., Jacobsen, A., Byrne, C.J., Heuer, M.L., Larsson, E., Antipin, Y., et al. (2012). The cBio cancer genomics portal: an open platform for exploring multidimensional cancer genomics data. Cancer Discov *2*, 401-404. 10.1158/2159-8290.CD-12-0095.
4. Gao, J., Aksoy, B.A., Dogrusoz, U., Dresdner, G., Gross, B., Sumer, S.O., Sun, Y., Jacobsen, A., Sinha, R., Larsson, E., Cerami, E., et al. (2013). Integrative analysis of complex cancer genomics and clinical profiles using the cBioPortal. Sci Signal *6*, pl1. 10.1126/scisignal.2004088.
5. Abida, W., Cyrta, J., Heller, G., Prandi, D., Armenia, J., Coleman, I., Cieslik, M., Benelli, M., Robinson, D., Van Allen, E.M., Sboner, A., et al. (2019). Genomic correlates of clinical outcome in advanced prostate cancer. Proc Natl Acad Sci U S A *116*, 11428-11436. 10.1073/pnas.1902651116.

6. Mandigo, A.C., Yuan, W., Xu, K., Gallagher, P., Pang, A., Guan, Y.F., Shafi, A.A., Thangavel, C., Sheehan, B., Bogdan, D., Paschalis, A., et al. (2021). RB/E2F1 as a master regulator of cancer cell metabolism in advanced disease. Cancer Discov. 10.1158/2159-8290.CD-20-1114.

7. Zhang, Y., Liu, T., Meyer, C.A., Eeckhoute, J., Johnson, D.S., Bernstein, B.E., Nusbaum, C., Myers, R.M., Brown, M., Li, W., and Liu, X.S. (2008). Model-based analysis of ChIP-Seq (MACS). Genome Biol *9*, R137. 10.1186/gb-2008-9-9-r137.

8. Chen, H., and Boutros, P.C. (2011). VennDiagram: a package for the generation of highly-customizable Venn and Euler diagrams in R. BMC Bioinformatics *12*, 35. 10.1186/1471-2105-12-35.

9. Ramirez, F., Dundar, F., Diehl, S., Gruning, B.A., and Manke, T. (2014). deepTools: a flexible platform for exploring deep-sequencing data. Nucleic Acids Res *42*, W187-191. 10.1093/nar/gku365.

10. Liu, T., Ortiz, J.A., Taing, L., Meyer, C.A., Lee, B., Zhang, Y., Shin, H., Wong, S.S., Ma, J., Lei, Y., Pape, U.J., et al. (2011). Cistrome: an integrative platform for transcriptional regulation studies. Genome Biol *12*, R83. 10.1186/gb-2011-12-8-r83.

11. Wang, S., Sun, H., Ma, J., Zang, C., Wang, C., Wang, J., Tang, Q., Meyer, C.A., Zhang, Y., and Liu, X.S. (2013). Target analysis by integration of transcriptome and ChIP-seq data with BETA. Nature protocols *8*, 2502-2515. 10.1038/nprot.2013.150.

12. Ritchie, M.E., Phipson, B., Wu, D., Hu, Y., Law, C.W., Shi, W., and Smyth, G.K. (2015). limma powers differential expression analyses for RNA-sequencing and microarray studies. Nucleic Acids Res *43*, e47. 10.1093/nar/gkv007.